CHAPTER 4
THE SPATIAL DISTRIBUTION OF GALAXIES

4.1 Introduction

Having looked at the properties of individual galaxies – both normal and active – in some detail, it is now appropriate to consider how these galaxies are distributed in space.

Surveys of the region outside our own Milky Way show that there are galaxies all around us. Deep field images such as those taken by the Hubble Space Telescope (Figure 2.40) have revealed that galaxies are present in great numbers out to very large distances. As suggested in Chapter 2, these galaxies are *not* distributed uniformly; there is structure present on all but the very largest distance scales.

At the smaller end of this range of scales, a proportion of galaxies are found in *groups* or *clusters*, which consist of local concentrations of tens to thousands of galaxies. Clusters of galaxies typically are no more than a few megaparsecs in diameter, but are themselves organized into larger structures called *superclusters* that can extend for tens of megaparsecs. On even larger scales, the matter in the Universe seems to resemble a three-dimensional network in which regions of high galaxy density are connected by *filaments* and *sheets*. These structures surround large *voids* in which very few galaxies are found. This appears to describe the current distribution of galaxies up to the largest observable scales.

In this chapter we will discuss how astronomers have come to their present understanding of the way in which galaxies, and more generally, matter is distributed throughout space. This has been one of the great scientific endeavours of the past fifty years or so, and is a process that continues with long-term projects that aim to produce accurate three-dimensional maps of vast regions of the Universe around us. We will look at some of these projects in detail and will also consider the efforts that are now being made to map the distribution of dark matter and tenuous intergalactic gas that pervades the Universe. Finally, we shall consider one of the techniques that astronomers use to describe the distribution of matter in the Universe – a process that is necessary if we are to come to an understanding of how cosmic structure was formed.

We start, however, by looking at the distribution of galaxies in our own neighbourhood.

4.2 The Local Group of galaxies

Our own Galaxy is a member of a small cluster – it belongs to a modest concentration of galaxies known as the **Local Group**. The Milky Way itself has about a dozen satellite galaxies, including two particularly prominent ones: the Large and Small Magellanic clouds. These irregular galaxies are visible to the naked eye as fuzzy patches in the southern sky (Figure 2.7b and c). (Note that images of many of the prominent members of the Local Group are given in Chapter 2.)

Slightly further away lies the largest of the Local Group galaxies – the Andromeda Galaxy or M31 (Figure 2.5). This spiral galaxy (type Sb) is somewhat more massive than the Milky Way and, at a distance of 0.8 Mpc, is the most distant object visible to the naked eye.

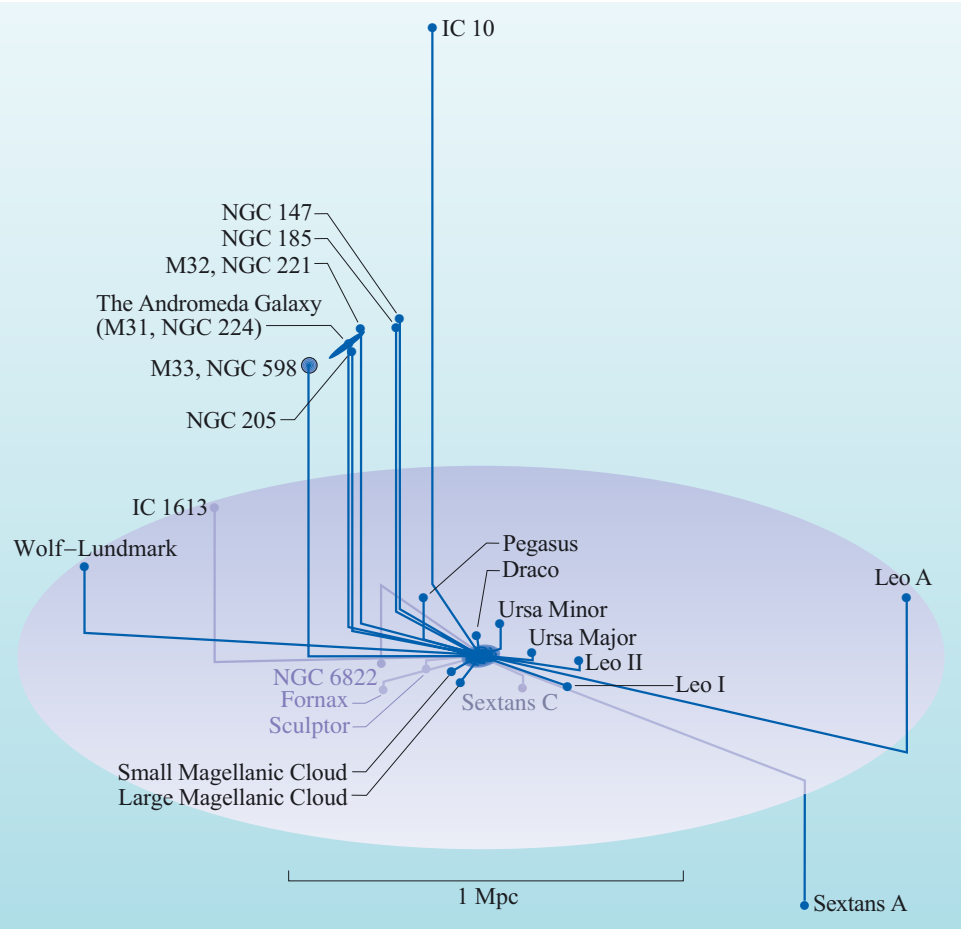

Figure 4.1 The main members of the Local Group of galaxies. Some are named after the constellations in whose directions they lie. In this diagram the Milky Way is located at the centre. (The disc separates the northern and southern halves of the celestial sphere.)

In total, the Local Group contains approximately 30 galaxies: Figure 4.1 shows how the main members of the Local Group are distributed in space.

The Local Group occupies a volume of space approximately 2 Mpc across. This is to be compared with the 0.03 Mpc diameter of the Milky Way. The Local Group is almost certainly not a transitory bunching of galaxies, but is **gravitationally bound**. Each member moves in an orbit determined by the gravitational influence of the whole Local Group. Furthermore, in a bound system, galaxies cannot normally escape unless ejected as the result of a collision between clusters or other perturbations.

Most of the members of the Local Group are much less massive than the Milky Way. After M31 and the Milky Way itself, the next most massive members of the Local Group are the two Magellanic Clouds and the more distant spiral galaxy M33 (Figure 4.2) – each having a mass approximately an order of magnitude less than that of the Milky Way. Of the remaining galaxies, most are dwarf elliptical galaxies with masses of typically just a few per cent of that of the Milky Way. M32 (visible in Figure 2.5 as a small galaxy just below the centre of the image) is a small companion of M31 and is classified as type E2 since it is slightly elongated. Leo I (Figure 2.8) is a dwarf elliptical at a distance of about 0.25 Mpc.

Dwarf ellipticals may be common but because they are very faint they are difficult to detect. Because of this we are uncertain of the exact number of galaxies in the Local Group; we have already noted that the current count is around 30, but it is

Figure 4.2 M33, a spiral galaxy in the Local Group. (D. Malin/IAC/RGO)

likely that further dwarf ellipticals will continue to be discovered as astronomical techniques improve. This difficulty in detecting faint objects has implications for deep surveys – as we look at more distant clusters, we see fewer of the less bright members. As clusters go, the Local Group contains only a small number of galaxies. Typically the term **group** is reserved for clusters with fewer than 50 members. The main characteristic of a **cluster** is that it is gravitationally bound and in this sense the terms 'group' and 'cluster' are interchangeable: the Local Group is simply a cluster with relatively few members. As will be seen in the next section, clusters can range from just a few members as in the Local Group, to much denser concentrations of thousands of galaxies.

4.3 Clusters of galaxies

Although the number of galaxies in a cluster can vary by a large factor, clusters do not vary so much in physical size: the typical cluster size of a few megaparsecs is not much different from the diameter of the Local Group. Thus *richer* clusters (those with more members) also tend to be more densely packed. Since we can observe galaxies out to distances of hundreds of megaparsecs, clusters are still very small structures on the overall scale of the observable Universe.

The most obvious way to study the distribution of galaxies is simply to photograph large areas of the sky and then to analyse the pattern of galaxies seen in the images. Historically, obtaining suitable images for such studies was a challenge: galaxies tend to be faint objects, so large aperture telescopes and long exposure times were required.

Technical difficulties aside, however, this approach is straightforward enough, and it has been applied since the 1930s. The first major survey was carried out by Harlow Shapley (Figure 1.27) who, together with Adelaide Ames in 1932, catalogued the positions of 1250 galaxies. The images taken by Shapley and Ames showed the first strong indication that galaxies are not distributed randomly in space: they found a number of compact regions containing significantly higher than average densities of galaxies. This survey thus provided early evidence for the clustering of galaxies.

Further surveys followed, adding more clusters to the total. Below we will discuss one of the most important – the Abell catalogue – in some detail. This survey is important because it was the first to introduce a classification scheme for clusters. More recent surveys have extended both the number of clusters discovered and the volume of space surveyed, but the Abell catalogue is still the starting point for astronomers embarking on a study of these objects.

Figure 4.3 shows images of two well-known nearby clusters – the Coma cluster, and the Virgo cluster.

These two examples illustrate some of the diversity and variety of clusters. The Coma cluster, which is at a distance of about 100 Mpc from our Galaxy, is a spherically symmetrical cluster consisting mainly of elliptical galaxies. By contrast, the Virgo cluster, which is about 20 Mpc distant, is much more irregular in shape, and contains a mixture of ellipticals and spirals. A feature that is common to both clusters however is the fact that each contains over a thousand galaxies.

Although clusters can contain many galaxies, it is important to appreciate that not all galaxies reside in clusters. In fact, the vast majority of galaxies exist outside of clusters. A galaxy that is not part of a cluster is called a **field galaxy**, and as we will see, care must be taken to identify and exclude these from cluster surveys.

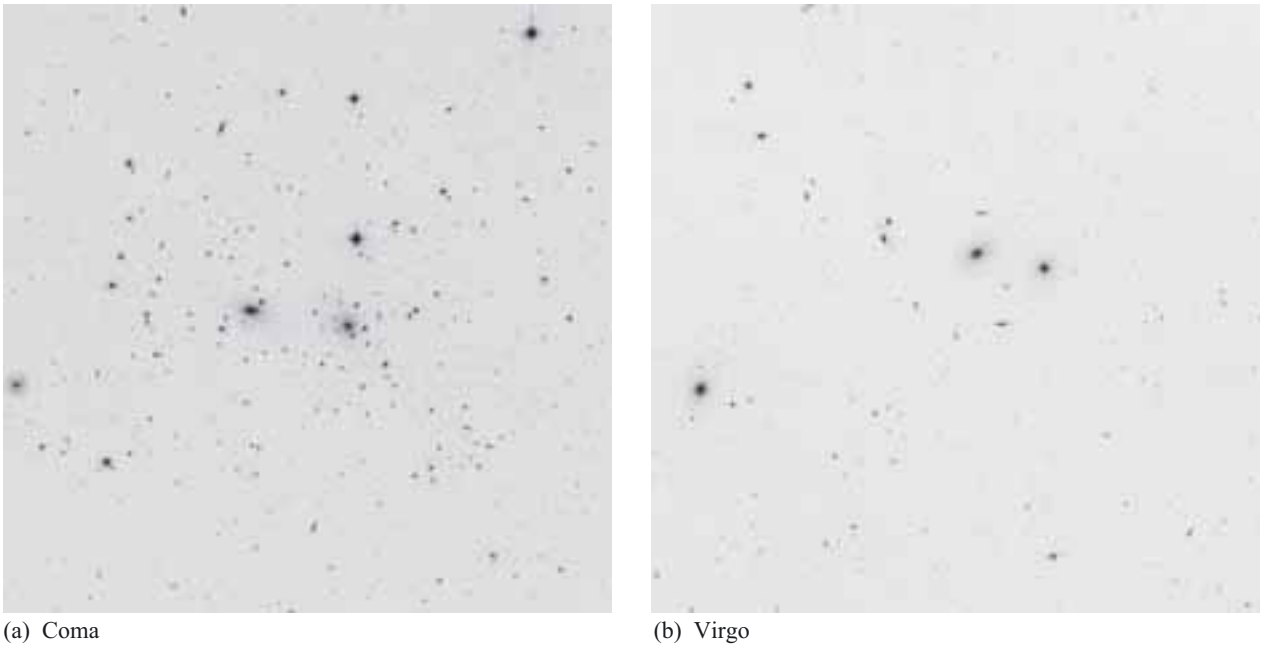

(a) Coma (b) Virgo

Figure 4.3 Optical images (visual band) of clusters of galaxies. (a) The Coma cluster of galaxies which lies at a distance of about 100 Mpc from our Galaxy. (b) The Virgo cluster of galaxies which is about 20 Mpc from the Milky Way. Both the Coma and the Virgo clusters of galaxies contain over a thousand galaxies. The fields of view of these images are relatively wide: $0.75° \times 0.75°$ in (a), and $2.5° \times 2.5°$ in (b). (Digitized Sky Survey/STScI)

4.3.1 The identification of clusters from imaging surveys

In 1958 George Abell (Figure 4.4) published a catalogue of 2712 clusters of galaxies which was the starting point for detailed study of these objects. In this section we will review the process by which Abell constructed this catalogue since it highlights some of the difficulties that have to be overcome by astronomers who endeavour to survey the Universe on large scales.

Abell's survey used plates taken using a special type of telescope called a Schmidt telescope (or Schmidt camera) that is well-suited to taking images that cover large areas on the sky. During the mid-1950s the 48-inch Schmidt telescope at the Mount Palomar Observatory (Figure 4.4) had been used to create a detailed photographic atlas of the sky. The images on these plates – each with a field of view just over 6 degrees square – together covered approximately 75% of the celestial sphere, including most of the northern sky and part of the southern. Abell used 879 of the 935 plates of the full survey as the basis for his search for clusters of galaxies. He examined the survey plates by eye to look for regions containing larger than average concentrations of galaxies. Later, he and his co-workers extended the catalogue to include more of the southern sky.

Abell's catalogue is significant because, for the first time, it contained a sufficiently large sample of clusters to allow a meaningful comparison of their different characteristics. The scale and extent of the survey also allowed the spatial distribution of clusters to be analysed for the first time.

Based on their visual differences, Abell was able to classify clusters according to various criteria. The most important of these is one which describes how many galaxies there are within a cluster. Abell called this property the **richness** of a

GEORGE OGDEN ABELL (1927–1983)

Figure 4.4 George Abell standing next to the Palomar 48 Inch Schmidt telescope. This design of telescope has a very wide field of view which facilitates the surveying of large areas of the sky. (California Institute of Technology)

George Abell (Figure 4.4) began his astronomical career as an observer on the Palomar Sky Survey (the survey on which his study of clusters of galaxies was based), and one of his early studies was to use the survey plates to examine low surface brightness planetary nebulae. Along with Peter Goldreich, Abell helped to establish the connection between these objects and the final stages of life of red giant stars.

For most of his career, he held a faculty position at the University of California, Los Angeles. He was an enthusiastic and popular teacher and subscribed to the view that in teaching science, it is more important to explain how we establish scientific knowledge than to simply present students with surprising or remarkable facts. He was committed to bringing science education to a broad audience: one example of this was his involvement in the production of a series of television programmes about relativity and cosmology in a collaboration between the Open University and the University of California.

cluster. Rich clusters are those that contain relatively high numbers of galaxies. However, as you saw in Chapter 2, it is difficult to detect faint galaxies, so a meaningful study of the number of galaxies in a cluster has to be based on the number of galaxies that exceed a certain threshold luminosity.

A vital piece of information that was needed in this process of detecting and classifying clusters was the distance of each. Abell had no direct means to measure the distances to all the galaxies in the survey, but he was able to use the apparent magnitudes of galaxies in a given cluster as the basis for estimating its distance. Specifically, he used the results of previous studies that indicated that the tenth brightest galaxy in each cluster should have about the same intrinsic luminosity. Thus the tenth brightest galaxy could be taken as a form of *standard candle*. This method did not allow Abell to calculate precise distances for each cluster – the values obtained were still very rough estimates. They were sufficient, however, to distinguish between clusters that were nearby and those that were more distant.

Abell's method of defining and selecting clusters was based on counting the galaxies within a circle of a certain radius on the photographic plate. Abell assumed that all clusters had roughly the same physical size: he estimated that clusters had a radius of about 2 Mpc. Subsequent studies have shown that this was a good assumption, and this 'standard' cluster radius is now known as the **Abell radius** R_A.

QUESTION 4.1

A cluster with an angular diameter of 1.9° is estimated to lie at a distance of 120 Mpc from the Earth.

(a) Calculate the diameter (in Mpc) of this cluster.

(b) What would the angular diameter of the same cluster be if it were at a distance of 420 Mpc?

Abell's work on defining clusters was very methodical – he was well aware that the presence of field galaxies and chance alignments between galaxies along a particular line of sight could give rise to spurious identifications of clusters. Since he wanted to minimize the number of false identifications in his catalogue he developed tests to identify clusters that are, to a high degree of statistical certainty, genuine associations of galaxies. The actual criterion used to define such a cluster was that the cluster must contain more than fifty members that exceeded a certain luminosity, and that these galaxies were located within a volume of space with radius R_A. Out of his original sample of 2712 suspected clusters, he identified 1682 cases which were statistically very likely to be genuine. Subsequent studies have shown that the vast majority of these objects are true clusters.

Abell also classified clusters of galaxies according to their symmetry, grading them on a scale running from *regular* to *irregular*. The regular clusters tend to be giant systems with spherical symmetry and a high degree of central concentration, and irregulars tending to be more open with low central concentrations and a significant amount of 'clumpiness' or sub-clustering.

Another type of study that can be based on imaging surveys relates to the morphogical types of galaxies that exist within clusters. It appears that the proportion of galaxies of different morphological type depends on the symmetry of the cluster. Regular

clusters such as the Coma cluster contain relatively few spiral galaxies, and are rich in lenticular and elliptical galaxies. This tendency is not exhibited by irregular clusters (such as the Virgo cluster), which seem to contain a higher proportion of spiral galaxies.

Abell's survey generated a number of interesting results: by adopting a methodical approach and introducing a classification scheme, Abell could do far more than merely catalogue the positions and richness of the clusters. He was also able to consider how the *distribution* of clusters – both over the surface of the sky and as a function of distance – might give information about the existence of larger scale structures.

One difficulty in mapping the distribution of clusters of galaxies is that it is not possible to observe the entire sky: external galaxies can only be seen in the part of the sky not obscured by our own Galaxy. This can be appreciated from maps that display the entire sky, such as Figure 4.5, which shows the positions of Abell clusters. Note that this map shows the celestial sphere in *equatorial* coordinates: the upper and lower halves of the map represent the northern and southern celestial hemispheres respectively. When a map of the celestial sphere is shown in such a way, the plane of the Galaxy snakes around the sky in an 'S'-shaped curve, as shown in the inset to Figure 4.5. It can be seen that only clusters that lie well away from the Galactic plane are visible.

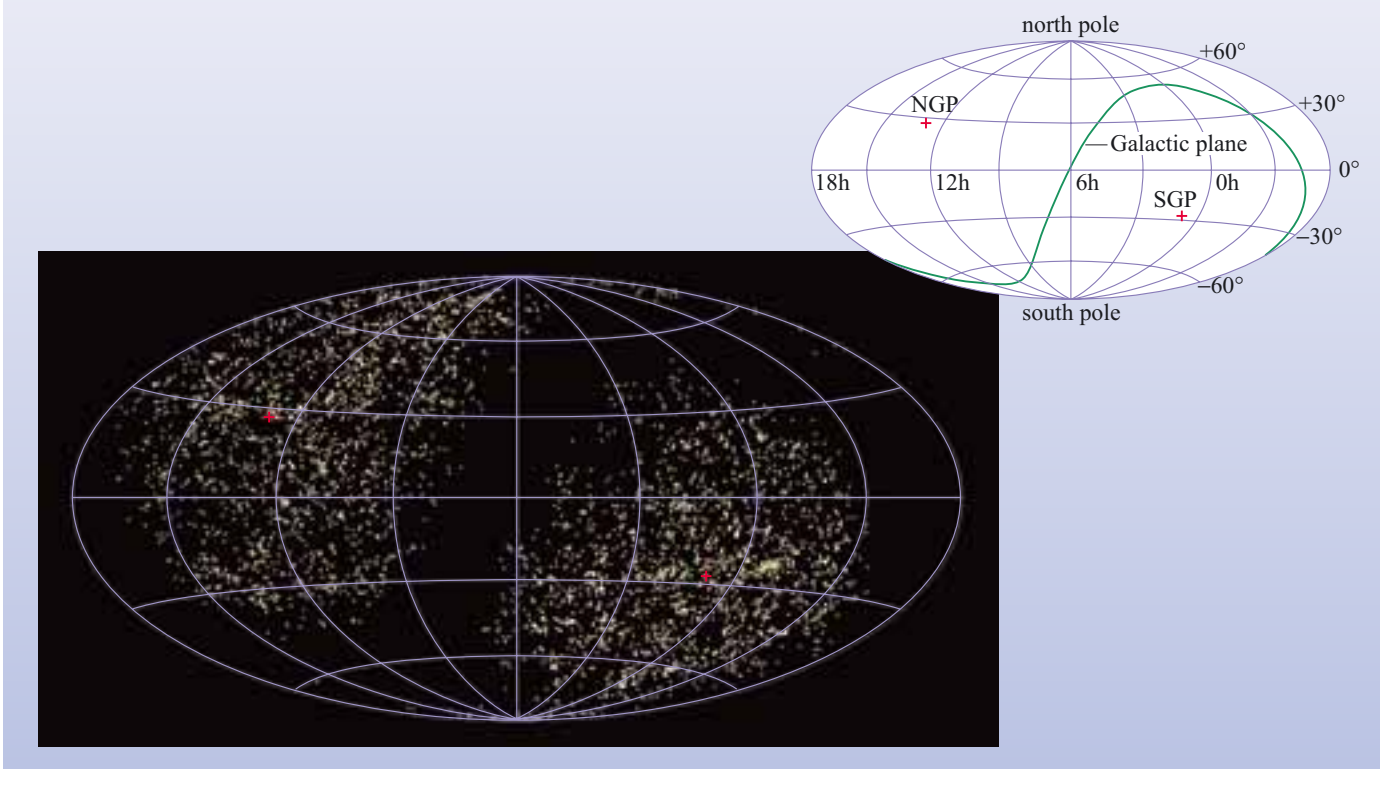

Figure 4.5 This map of the whole sky shows the distribution in equatorial coordinates of Abell clusters. Note that no clusters can be observed close to the Galactic plane because of obscuration due to the interstellar medium of the disc of our Galaxy. (The clusters are those identified in Abell's 1958 study of the northern hemisphere, and a similar study of the southern hemisphere that was published by Abell, Corwin and Olowin in 1989.) The red crosses show the North Galactic Pole (NGP) and the South Galactic Pole (SGP).

As mentioned above, another difficulty was that it was only possible for Abell to make rough estimates of distance. Modern redshift measurements together with improvements in the determination of the Hubble constant have allowed distances to clusters to be determined much more accurately. Within these constraints it was nevertheless possible to reach some overall conclusions on cluster distribution. Abell did not find much variation in the distribution of clusters with distance – there were just as many clusters at large distances as at smaller distances. Looking at the distribution *across* the sky, however, it was apparent that clusters are themselves *not* scattered randomly: although clusters were found in all parts of the observable sky their distribution, as can be seen from Figure 4.5, is far from uniform. Abell's data therefore suggested the existence of structure on larger scales than individual clusters.

QUESTION 4.2

The most distant Abell cluster has a redshift of 0.25. How far away is this cluster? (Assume that $H_0 = 72\ \mathrm{km\ s^{-1}\ Mpc^{-1}}$.)

More recent surveys have probed out to much greater distances than Abell's catalogue. As we look out to greater and greater distances from the Earth, galaxies become fainter, but they also become more numerous. For both these reasons it has become impractical to carry out such surveys by manual inspection of photographic plates, and modern surveys usually use computer-based methods in which digital images are analysed automatically.

Photographic and digital imaging surveys have catalogued many thousands of clusters and clearly shown that galaxies are not distributed randomly. But this type of survey has some limitations. In particular, imaging surveys are essentially *two-dimensional*: they show the positions of the galaxies as projected onto the celestial sphere but do not directly provide information on the *distance* from the Earth.

Space, however, is of course three-dimensional. In order to build up a clear picture of the large-scale structure of the Universe it is necessary to add *accurate* distance information to the two-dimensional position information. This allows a fully three-dimensional map to be built up showing the volume distribution of galaxies throughout space. More recent surveys are doing exactly this, and the techniques and results will be described in Section 4.4.

In order to work towards the ultimate aim of understanding how clusters form and evolve, it is necessary to learn something about the physical properties of clusters such as mass and composition, and it is to these two aspects of clusters of galaxies that we now turn.

4.3.2 The masses of clusters of galaxies

In common with most astronomical objects, it is the total mass of a cluster of galaxies that is the single most important physical property that astronomers are interested in determining. Once the mass of a cluster is known, it becomes possible to understand the gravitational influence that the cluster has on its environment. Furthermore, knowledge of the total mass of the cluster will allow estimates to be made of the relative proportions of luminous and dark matter.

Mass, however, is not a property that can be directly measured: instead it has to be inferred from measurements of observable quantities – such as the wavelengths of spectral lines. The following three sections describe different methods of determining the masses of clusters of galaxies. Although these techniques are based on different physical effects, it is found that all three give very similar answers for the cluster masses.

Estimation of cluster masses using velocity dispersion

In Chapter 2 you learned about the *virial theorem*, which is used to determine the masses of galaxies. The virial theorem states that the magnitude of the total gravitational potential energy of a bound system is equal to twice the total kinetic energy. In this way, the distribution of *velocities* (which is related to the kinetic energy) can be related to the overall *mass* of the system (which is related to the gravitational potential energy).

Clusters are collections of galaxies rather than stars, but the same principle applies – individual galaxies within a cluster will move under the influence of the gravitational field of the total mass in the cluster. The significance of this is that the velocities of galaxies within a cluster are observable quantities – they can be measured using Doppler shifts and this gives us a method for estimating the total cluster mass.

This is exactly the same principle as the method described in Chapter 2, Section 2.3.2 for determining the masses of elliptical galaxies using the velocity dispersion of individual stars within the galaxy. In the case of clusters, the only modification is that it is the velocity dispersion of galaxies within the cluster that is used rather than that of stars within a galaxy.

■ What assumptions need to be made for the virial theorem to hold?

❑ The system must be virialized – the cluster must be in a steady state – neither expanding nor contracting and the distribution of velocities of the galaxies must be unchanging. (See Box 2.1.)

When it first begins to form, a cluster may be far from being virialized. Over time, collisions and other interactions between the individual galaxies, gas and dark matter within the cluster will cause their energy to be redistributed. Eventually the motions will settle down into a steady state where further interactions do not change the distribution of kinetic and potential energies. This state is sometimes referred to by describing a cluster as being *relaxed* or in a state of *dynamic equilibrium*. Some clusters – especially those which show a high degree of symmetry are thought to be virialized. Clusters which appear irregular are far less likely to have reached this state, and so it may not be appropriate to apply this method of mass determination in such cases.

The redshifts of galaxies within clusters can be used to determine their velocities in the radial direction (i.e. along the line of sight). As for the case of stars within elliptical galaxies (Chapter 2) the kinetic energy can be characterized by the velocity dispersion. Then the mass of the cluster is given by:

$$M \approx \frac{R_A (\Delta v)^2}{G} \qquad (4.1)$$

where R_A is the Abell radius and Δv the dispersion in the line of sight velocities of the cluster members.

Clearly, it is important to ensure that only galaxies belonging to the cluster are included. Care must be taken to ensure that foreground or background galaxies along the line of sight are identified and excluded from the velocity dispersion measurements.

QUESTION 4.3

In the Virgo cluster the (elliptical) galaxies show a velocity dispersion Δv of 550 km s^{-1} (this value is given to a precision of 2 significant figures). Calculate the mass of this cluster. Express your answer in solar masses.

The Swiss-American astronomer Fritz Zwicky was the first to apply the virial theorem, using it in the 1930s to estimate the mass of the Coma cluster. Surprisingly, he found that the mass was much larger than the sum of the masses of the individual member galaxies. Historically, this was one of the first indications of the presence of dark matter in the Universe.

We saw in Chapters 1 and 2 that there is evidence for the existence of dark matter within our Galaxy and other galaxies. The results of studies of the masses of clusters of galaxies indicate that a cluster as a whole must include a large amount of dark matter surrounding the galaxies. The conclusion that has been reached is that the luminous matter in clusters accounts for only a small proportion of the mass, with the remaining 70% to 90% of the total cluster mass provided by dark matter.

FRITZ ZWICKY

Figure 4.6 Fritz Zwicky (1898 – 1974). (California Institute of Technology)

Fritz Zwicky (Figure 4.6) was born in Varna, Bulgaria of Swiss parents. He studied in Switzerland and retained his Swiss nationality even when he moved to California Institute of Technology (Caltech), USA in 1925.

Zwicky originally trained as a crystallographer but became interested in the advances being made in astronomy at Caltech and nearby observatories. He remained professor of astronomy at Caltech until he retired in 1968. Zwicky was full of self-belief and came up with a lot of revolutionary ideas, largely intuitively.

His work on clusters of galaxies led to the idea of the existence of large amounts of dark matter in the Universe. Not only was Zwicky the first to infer the presence of dark matter but he also went on to suggest that the *gravitational lensing* of background galaxies would be the most direct way to probe the dark matter in the Universe. (As we will see in Section 4.5, such techniques are now being developed.)

Cluster mass from X-ray emission

Clusters of galaxies are not only visible in the optical part of the spectrum: they also produce strong X-ray emission. In 1971, results from the pioneering X-ray satellite Uhuru, confirmed what had been suspected from X-ray measurements made from sounding rockets – that clusters of galaxies are among the brightest X-ray sources in the sky. This X-ray emission arises from a vast quantity of very hot gas (typically at temperatures of between 10^7 to 10^8 K) that pervades the intergalactic space within the cluster.

In recent years, advances in X-ray astronomy have allowed clusters to be identified from X-ray surveys, often more efficiently than using optical imaging methods. Optical observations of clusters suffer from the problem of distinguishing true members of a cluster from other galaxies that are not associated with the cluster, but which happen to lie along the same line of sight. This is much less of a problem for X-ray observations because there are far fewer X-ray sources that could be incorrectly attributed to emission from a cluster. A cluster appears as an extended region of diffuse X-ray emission (Figure 4.7) that shows no variability with time. Other extragalactic sources of X-ray emission are normal and active galaxies and these are quite distinct from clusters of galaxies. As you saw in Section 3.2.2, normal galaxies typically have very low luminosities at X-ray wavelengths. Active galaxies, which can be luminous X-ray sources, are unresolved sources (i.e. point-like) that are often variable.

So how are the X-rays produced? Closer examination reveals that the X-rays from clusters form a broad continuous spectrum, with some emission lines (which we will discuss later). The broad continuous spectrum is characteristic of a mechanism known as **thermal bremsstrahlung**, which is normally associated with very hot ionized gas (Box 4.1, overleaf).

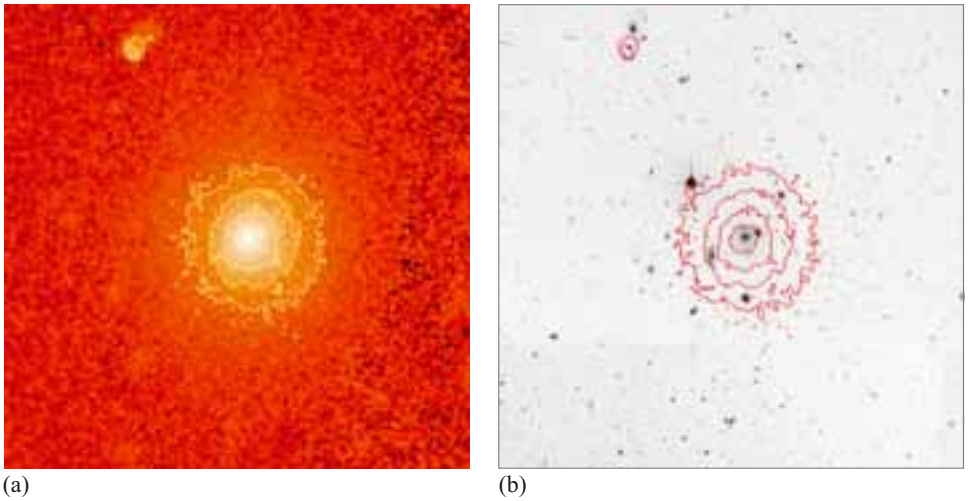

(a) (b)

Figure 4.7 A comparison of optical and X-ray images of Hydra A, a cluster of galaxies that is about 280 Mpc from Earth. (a) An X-ray image of Hydra A, as observed using the ROSAT X-ray Observatory. The image shows the emission from a large cloud of gas, several Mpc across that is at a temperature of about 3×10^7 K. (b) An optical image in the visual waveband of the Hydra cluster (shown as a photographic negative), with contours of X-ray emission overlaid. It can be seen that the hot X-ray emitting gas fills the space between the galaxies in the cluster. (Both (a) and (b) show the same field of view, and have an extent of $1° \times 1°$.) ((a) NASA; (b) Optical data from the Digitized Sky Survey/STScI)

BOX 4.1 THERMAL BREMSSTRAHLUNG

Thermal bremsstrahlung is an X-ray emission mechanism that typically takes place in a high-temperature, low-density plasma. As a free electron passes close to an ion in the gas it is deflected (Figure 4.8) without being captured. As a result of this acceleration the electron emits a photon while at the same time losing a corresponding amount of kinetic energy and slowing down a little.

X-rays generated in this way are known as *bremsstrahlung* (a German word that means *braking* or *deceleration* radiation). This type of X-ray emission is also called *free-free* emission because the electron moves freely both before and after the encounter with the ion.

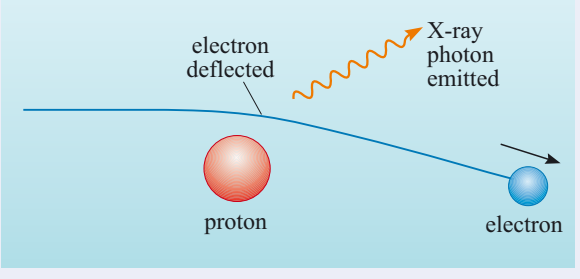

Figure 4.8 Mechanism for Bremsstrahlung emission

The energy ε_{ph} of a photon generated by this process depends on the average thermal energy of the electrons and is given approximately by:

$$\varepsilon_{ph} \sim kT$$

where k is the Boltzmann constant ($1.38 \times 10^{-23}\,J\,K^{-1}$) and T is the temperature of the gas. It is common in X-ray astronomy to express photon energies in terms of kilo-electronvolts ($1\,keV = 1.60 \times 10^{-16}\,J$). Photon energies in the range 1 to 10 keV are typical for X-ray clusters, corresponding to temperatures of about 10^7 to 10^8 K.

Because the X-rays are produced by the acceleration of *free* electrons, the spectrum of bremsstrahlung emission is a smooth continuum (Figure 4.9). This is characteristic of a fully ionized gas where the electrons are not bound to individual atoms. Bremsstrahlung spectra are thus distinct from the *line spectra* which are produced when electrons make transitions between the energy levels of atoms.

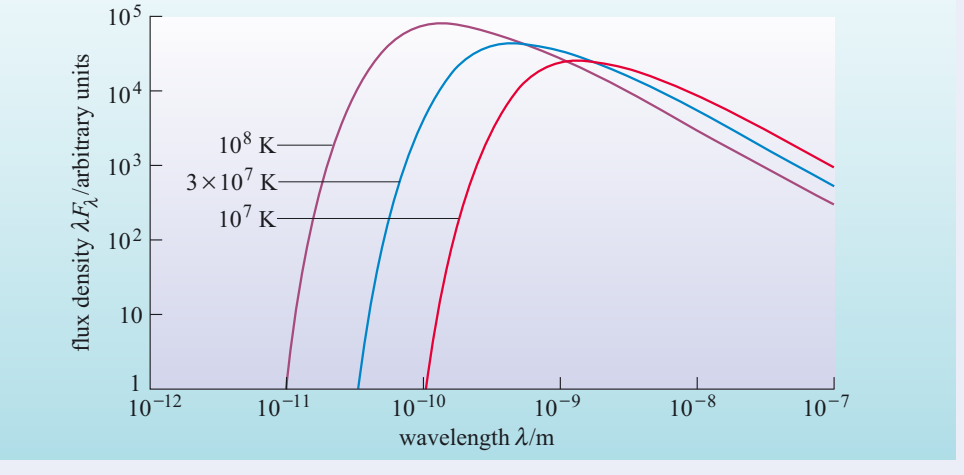

Figure 4.9 The spectral energy distribution due to hot gas (at three temperatures as indicated) emitting by the mechanism of thermal bremsstrahlung. Note the broad continuous spectrum that peaks at shorter wavelengths for higher gas temperatures.

The presence of bremsstrahlung X-ray emission is evidence for the presence of large quantities of hot ionized gas within the cluster. This gas is predominantly composed of hydrogen and helium, although it does contain a small fraction of heavier elements. As can be seen from Figure 4.7b this hot **intracluster medium** or **ICM**, is present between the galaxies, permeating the cluster out to a radius of a few megaparsecs. This makes clusters appear as extended, diffuse areas of X-ray emission.

With the benefit of X-ray images, our view of a typical cluster now becomes a large cloud of hot (10^7–10^8 K) ionized gas with the galaxies embedded in it.

- The temperature of the intracluster medium at the centre of a cluster is typically around 10^7 to 10^8 K – similar to that found at the centre of the Sun. Why, then, do we not see strong X-ray emission from the hot plasma within the core of the Sun and other stars?
- X-rays generated in the core of a star do not escape directly: in the dense environment of the solar interior, photons are repeatedly scattered and reach thermal equilibrium with matter. Eventually, the energy that was originally in the form of X-ray photons escapes from the outer layers of Sun – the relatively cool photosphere – at ultraviolet, visible and infrared wavelengths.

Although the total mass of gas in a cluster is much larger than that of the Sun, it is spread out over a vast volume of space (2 Mpc compared to one solar radius). The overall density of the ICM is therefore many orders of magnitude lower than the density of material in a star, and this allows the X-rays to escape. In this respect the intracluster gas is similar to the tenuous gas in the Sun's corona – although it should be noted that intracluster gas is many orders of magnitude less dense than gas in the solar corona.

To appreciate how this X-ray emission can be used to estimate the mass of a cluster it is necessary to consider how the intracluster gas supports itself. An important idea here is the concept of *hydrostatic equilibrium* similar to that used to model the stability of a star. A spherical region of gas will tend to collapse under the influence of its own gravity. In the case of a cluster, the gravitational field is produced not only by the mass of the gas itself, but also by the mass of the galaxies in the cluster, together with the mass of any dark matter.

The ICM will be supported against this gravitational collapse by the pressure of the gas. In equilibrium, the pressure changes with distance from the centre of the cluster in a way that exactly balances the effect of gravity. The temperature and density of intracluster gas can be measured from X-ray observations. The pressure of the gas can be calculated once the temperature and density are known, and by using the relationship that balances gravity against the pressure gradient, the total mass of the cluster can be inferred.

The cluster masses that have been obtained from X-ray observations are typically much higher than the mass that can be accounted for by the galaxies and intracluster gas alone. For a given temperature, pressure gradients within the ICM are *higher* than expected. This suggests that the gravitational field within the cluster is *stronger* than that provided by the mass of the galaxies and intracluster gas alone. Total cluster masses of 10^{14} to $10^{15} M_\odot$ are typical.

Again, this is much greater than the mass that can be accounted for by the galaxies in the cluster – which only constitute about 10% of the total mass. Furthermore, X-ray observations also allow an estimate to be made of the mass of gas in the intracluster medium and this is typically found to account for between 10% and 30% of the total mass of a cluster. The remaining mass is believed to be made up mainly of dark matter.

Cluster mass from gravitational lensing

A completely different approach to measuring cluster masses is based on the effect that gravity has on light. Einstein's general theory of relativity makes a number of predictions. One of these predictions is that, in addition to affecting the paths of objects such as planets, gravity can also affect light: the path of light will be bent if it passes close enough to a sufficiently massive object. This prediction was confirmed in 1919 by an expedition to the island of Principe, off the coast of West Africa, led by Sir Arthur Eddington. By measuring the positions of stars during a total solar eclipse (Figure 4.10), the bending of starlight passing close to the surface of the Sun was measured and found to be in agreement with Einstein's theory.

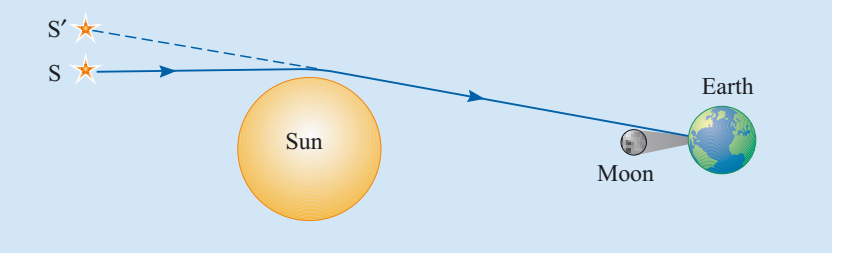

Figure 4.10 A schematic illustration of an eclipse observation of the gravitational bending of starlight. In order to be deflected by a significant amount, a ray of light from a distant star must pass very close to the surface of the Sun. Normally it would not be possible to see this effect, but during an eclipse the Moon obscures the extremely bright solar disc, allowing stars to be observed close to the limb of the Sun. Light from star S is deflected by a small amount, making its position appear to shift to S′.

This bending of light is a weak effect: Eddington's measurement was only possible when light passed very close to the surface of the Sun, and even then the angular deviation of just 1.74 arcsec was so small as to be barely measurable.

The deflection of rays of light becomes larger as the mass of the deflecting object increases. Since a cluster of galaxies typically has a high mass, we might expect that it could act as a **gravitational lens** and bend the paths of light rays from an object lying behind it, as shown in the simple arrangement in Figure 4.11. Rays of light from the galaxy at position S are deflected as they pass close to the cluster, and the observer at O, sees an image at position I. As well as this change in apparent position, the gravitational lens also causes the image of the background galaxy to be distorted, and typically produces multiple images.

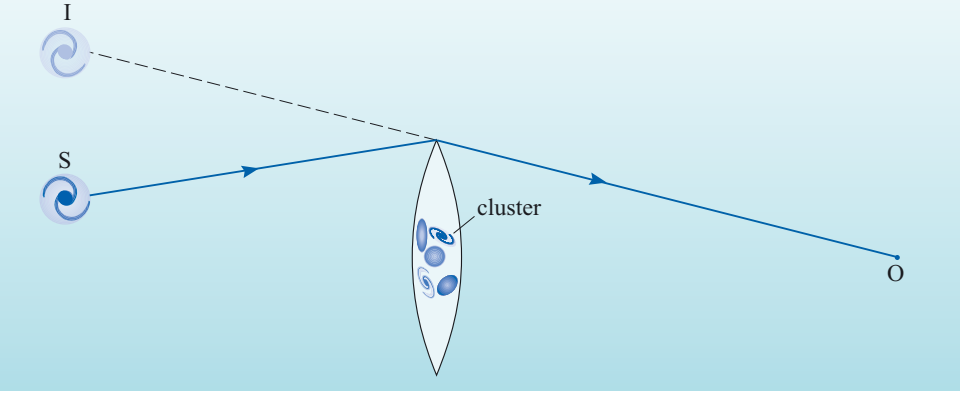

Figure 4.11 Schematic diagram of a gravitational lens. Light from the distant galaxy S is deflected as it passes a cluster of galaxies, causing a distorted image of the original galaxy to appear at I. Depending on the distribution of mass in the cluster, several images may be formed in different positions.

To date, over 50 cases of gravitational lensing have been observed. In addition to causing multiple or distorted images, gravitational lenses can also increase the apparent brightness of distant objects, in much the same way as a conventional lens focuses light. By concentrating light in this way, one effect of gravitational lensing is that it allows observation of distant objects which would normally have been too faint to be seen. One example of this is shown in Figure 4.12. Lensing in the cluster CL0024+1654 has produced five images of a more distant galaxy. The images of this galaxy are seen as blue elongated rings, one near the centre of the image and four others further out.

How can gravitational lensing be used to measure the masses of clusters of galaxies? Clearly the amount of distortion seen will depend in some way on the mass of the cluster that is acting as a lens. Calculating the exact distribution of mass in the lensing cluster can be quite difficult: just as with a glass lens, the exact shape of the lens will determine the nature of the image distortion and magnification. In cases like CL0024+1654 the pattern of distortions is very complicated – rather like looking at the distant galaxy through the bottom of a glass bottle.

In order to make reliable estimates of cluster mass, we need to look for simpler situations. Occasionally the multiple images resulting from gravitational lensing form symmetrical arcs surrounding the centre of the lensing cluster. A particularly spectacular example of this can be seen in the cluster Abell 2218 (Figure 4.13).

Figure 4.12 Lensing by CL0024+1654. Several distorted images of a distant blue galaxy can be seen encircling the yellower galaxies within the cluster. Analysis of these distorted images suggests that the background galaxy has an unusual shape. This may indicate that the distant galaxy is in the process of forming, or merging with another galaxy. (W. N. Colley and E. Turner (Princeton University), J. A. Tyson (AT & T Bell Labs, Lucent Technologies) and NASA)

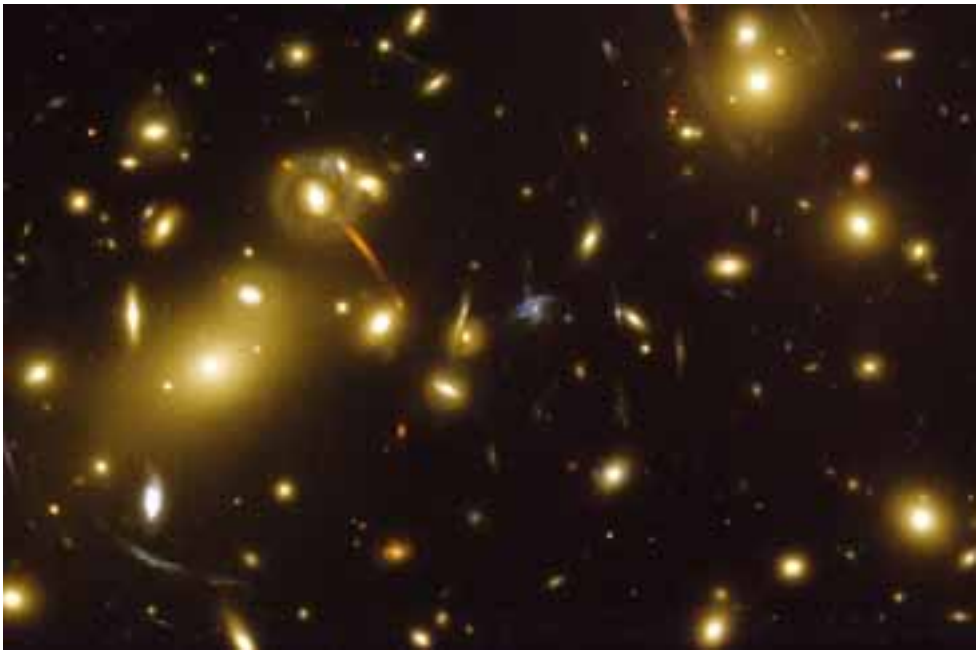

Figure 4.13 Gravitational lensing in Abell 2218. Note the arcs of concentric circles formed by the lens. (NASA, ESA, R. Ellis (Caltech) and J.-P. Kneib (Observatoire Midi-Pyrenees))

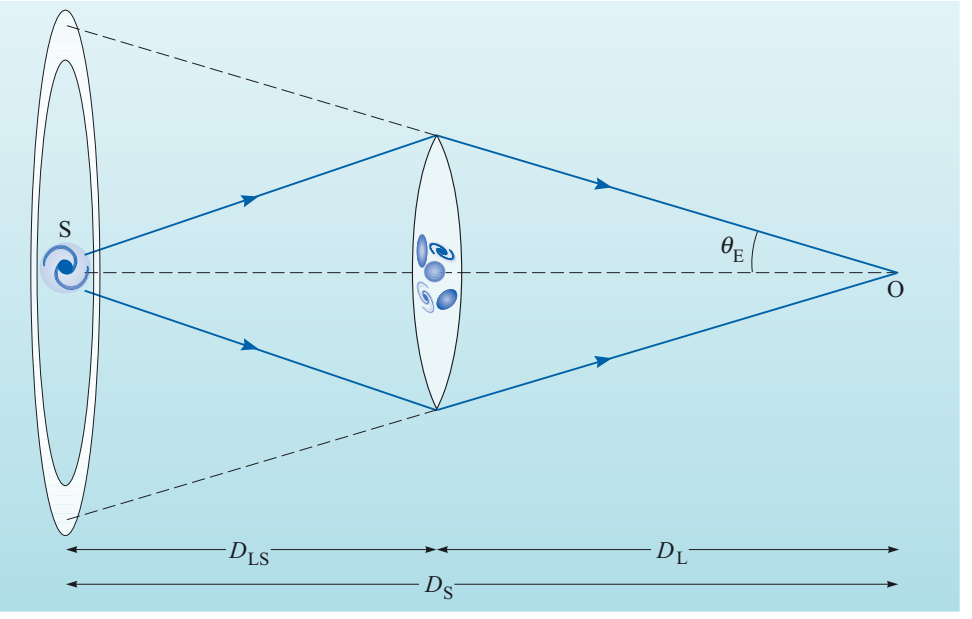

Figure 4.14 The geometry of a source imaged as a ring with angular radius θ_E.

Figure 4.14 shows a schematic view of this type of lensing situation. Here the distribution of mass in the lensing cluster is symmetrical and concentrated at the centre. The distant galaxy S is located exactly along the centreline. The paths of light rays passing either side of the cluster are distorted equally, resulting in symmetrical rings or arcs similar to those seen in Abell 2218.

If the alignment of source and lens is perfect, then the resulting image takes the form of a complete ring surrounding the lens. Such a ring is known as an **Einstein ring** and several examples like the one shown in Figure 4.15 have been discovered.

Figure 4.15 The Einstein ring B1938+666 as observed with the Hubble Space Telescope. In this case the foreground lens is a galaxy seen as the bright spot in the centre. (L. J. King (University of Manchester) and NASA)

- For a given cluster-to-source distance, how would you expect the angular radius of the Einstein ring to depend on the mass of the lensing cluster?

- The greater the mass of the cluster, the more the path of the light rays would be bent. So a more massive cluster would produce a ring of greater angular radius.

For the situation shown in Figure 4.14, the image of the distant object would appear as a complete ring with an angular radius θ_E that is given by:

$$\theta_E = \sqrt{\frac{4GM}{c^2}\frac{D_{LS}}{D_L D_S}} \qquad (4.2)$$

Where D_S is the distance between the observer and the distant source galaxy, D_L is the distance from the observer to the gravitational lens, and D_{LS} is the distance from the gravitational lens to the source.

Using Equation 4.2, the mass M of the lensing cluster can be estimated. (Note that similar calculations can be carried out for the less symmetrical situations where the lensing has not produced a complete ring.)

QUESTION 4.4

The largest lensed arcs in the image of Abell 2218 shown in Figure 4.13 have an angular radius θ_E of approximately 1.0 arcmin. This cluster is one of the most distant in the Abell catalogue: with a redshift of $z = 0.17$, it lies at a distance of approximately 700 Mpc from Earth. Using these values, and assuming that Equation 4.2 can be applied to this gravitational lens, estimate the mass of Abell 2218 in solar masses. Assume that the cluster is mid-way between the distant background galaxies and the Earth.

Gravitational lensing has an advantage over the other methods discussed in that it relies just on the distribution of mass within the cluster – we don't have to make assumptions about virialization or hydrostatic equilibrium. Of course, since lensing is a direct result of the gravitational field, it is sensitive to *all* the mass in the cluster, whether from galaxies, gas or dark matter.

Masses of clusters estimated from gravitational lensing lie within the range of 10^{14} to $10^{15} M_\odot$. This is consistent with the other two methods of mass determination and once again suggests the presence of significant quantities of dark matter within clusters.

4.3.3 The composition of clusters

As we have seen, cluster masses can be estimated by three independent methods: velocity dispersion, X-ray emission, and gravitational lensing. The results from these methods are all roughly consistent, typically agreeing within a factor of two or three. Typical masses range from less than $10^{14} M_\odot$ for the smallest clusters and groups to $10^{15} M_\odot$ for the richest clusters. Furthermore, the fact that three different techniques based on completely different physical principles are in such good agreement is compelling evidence for the existence of dark matter.

In addition to measuring mass, these three methods also enabled us to learn something about the different constituents of a cluster – galaxies, gas and dark matter. The results suggest that only a small percentage of the total mass of a cluster is contained in the galaxies themselves, with about 10%–25% in the intracluster medium, and the remaining 70%–90% as dark matter (see Table 4.1). The picture that has emerged is of a diffuse cloud of gas and dark matter which surrounds the galaxies and permeates the space between them.

Table 4.1 Relative contributions to the total mass of a cluster of galaxies due to its three major constituents.

Constituent	Contribution to total mass
galaxies	<10%
intracluster gas	10–25%
dark matter	70–90%

As described in Chapter 2, each individual galaxy has it own complement of gas (in the form of *interstellar* medium) and dark matter. We could therefore think of a cloud of gas and dark matter filling the whole cluster, with individual denser haloes around each galaxy. The density of material is highest around and within the member galaxies, but the large volume of the cluster compared to that of the galaxies means that the intracluster gas and dark matter – spread between individual galaxies – makes up most of the total mass of the cluster.

4.3.4 The formation and evolution of clusters

The study of the evolution of clusters is still in its infancy. As is the case in the study of the evolution and formation of galaxies (Chapter 2), the study of the evolution and formation of clusters takes the approach of trying to match simulations of the formation of structure to observations of the evolution of these objects.

The scenarios for the formation of structure that were described in Chapter 2, should also be scenarios that produce clusters as a natural outcome. As you saw in Chapter 2, the preferred scenario for the formation of structure is a hierarchical model in which small-scale structures (such as galaxies) form before larger ones (such as clusters).

The observational approach to studying the evolution of clusters is, at present, not well developed, but some advances are being made. For the remainder of this section we shall consider some of the results from studies of cluster evolution that may eventually help to confirm whether the scenarios of structure formation are correct.

The evolution of galaxies within clusters

We can start by looking at the evolution of galaxies within clusters. As noted earlier, clusters all have roughly the same size, with most of the galaxies being contained within the Abell radius of about 2 Mpc. The total number of galaxies within a cluster can vary greatly however, and it therefore follows that the density of clusters can also vary to a great extent. The richest clusters may contain hundreds of galaxies within the 2 Mpc radius, and towards the centres of such clusters the galaxies will be packed very densely.

■ What processes affecting the evolution of galaxies might depend on the density of packing of galaxies within a cluster?

❑ In the denser environments of rich clusters, there is more opportunity for collisions between galaxies.

During mergers the discs of spiral galaxies can be destroyed. Earlier it was mentioned that richer clusters tend to contain fewer spiral galaxies and a larger proportion of ellipticals. Such an observation seems consistent with the idea that rich clusters are an environment in which there have been many collisions and mergers of galaxies.

The role of mergers in cluster evolution

We have seen that within clusters, galaxies can collide and merge. What about the clusters themselves? Is there any evidence that clusters have built up from mergers of smaller clusters?

We can start by looking for evidence that mergers between clusters do actually occur, and to do this we have to make use of X-ray observations. Earlier, we saw how the strong X-ray emission from the hot intracluster gas can be used in estimating cluster masses. We can study the structure of the intracluster medium by looking at another aspect of the X-ray emission: in addition to the continuous thermal bremsstrahlung described in Box 4.1, the X-ray spectra of many clusters also contain *emission lines*, which signify the presence of elements heavier than hydrogen and helium.

As mentioned earlier, the intracluster medium consists mainly of hydrogen and helium. Why do line features in the spectra indicate that other, heavier, elements must also be present in the intracluster medium? The answer lies in *ionization energies*.

At temperatures of 10^7 to 10^8 K, hydrogen is fully ionized – that is, the electrons are completely separated from the hydrogen nuclei. Helium is also fully ionized at these temperatures. It is the free electrons in this plasma that give rise to the continuous bremsstrahlung emission. Being fully ionized, the hydrogen and helium will be not be able to produce line spectra, which come about as a result of transitions between energy levels within atoms.

It takes much more energy to remove all the electrons from the atoms of heavier elements such as iron: even at 10^8 K such atoms are not completely ionized. Any atoms of these elements will be present in the form of partially ionized atoms which have lost only some of their electrons. Transitions involving the tightly bound inner electrons in these ions give rise to line spectra in the X-ray part of the electromagnetic spectrum. Each element has its own characteristic spectral lines and this allows the presence of specific elements to be confirmed.

- Elements heavier than hydrogen and helium – were not present in the primordial material from which the first stars and protogalaxies would have condensed. How could the intracluster medium have become enriched with these heavy elements?

- An early period of star formation within the galaxies of the cluster might have included many massive short-lived stars which ended their lives as supernovae. Material expelled from supernovae contains heavy elements, and shockwaves from the explosions could propel this material out of the galaxies thus enriching the intracluster medium with elements heavier than hydrogen and helium.

Further information on the physical properties of the intracluster medium can also be obtained from looking at the line emission X-ray spectra of specific elements. The line spectrum of *iron* in particular is very useful: measurements of the relative strengths of emission lines in the iron spectrum can give a much more precise measurement of temperature than can be obtained from the broad continuous bremsstrahlung spectrum of a cluster. This allows detailed maps of the temperature distribution within clusters to be produced.

A very interesting result from such maps is that many clusters do not have the smooth temperature distribution which would be expected if the clusters were in hydrostatic equilibrium.

Figure 4.16 shows observations (made with the Chandra X-ray observatory) of the cluster Abell 2142 that suggest that this cluster has undergone merger events. Firstly, the map of X-ray surface brightness (the contours in Figure 4.16a) shows that the cluster has sharp edge towards the upper right-hand side (this is where the contours are packed closely together). This edge is believed to be the shock front that resulted from the merger of two clusters. Secondly, the temperature map of the X-ray emitting gas (Figure 4.17b) shows substantial variation across the cluster. The regions of cooler gas in the centre of the cluster (the blue central region in Figure 4.17b) are interpreted as the dense cores of subclusters that have survived merger shockwaves. Thus, unusually, Abell 2142 has a cooler core surrounded by hot, shocked gas.

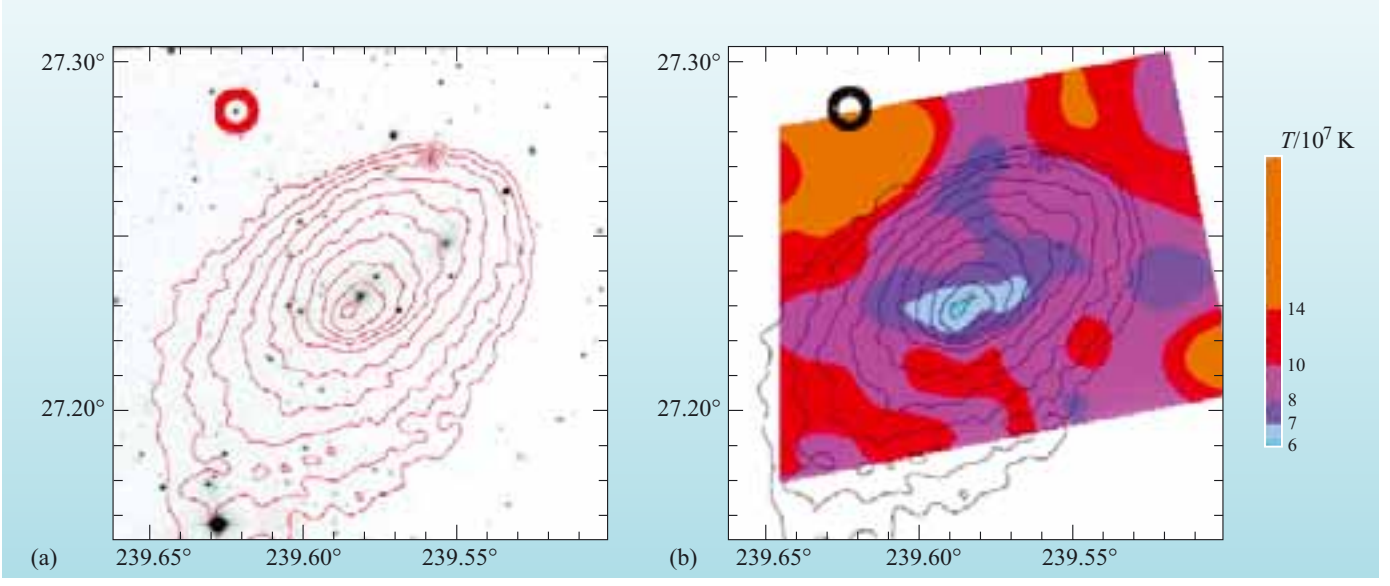

Figure 4.16 Observations of the cluster Abell 2142 which is possibly undergoing a merger event. (a) An optical image with the X-ray surface brightness contours overlaid. (b) A temperature map of the central region of the cluster with overlaid X-ray surface brightness contours. The central region is colder than the surrounding shocked region. (Markevitch *et al*., 2000)

These findings support the view that clusters appear to grow by the merger of smaller *subclusters* which are small concentrations of galaxies. Temperature maps indicate that this is an ongoing process in many clusters, where hot and cold regions are related to the shocks and other processes which occur as a result of the infall of subclusters. In some places, cold features within the intracluster medium have been identified with regions where subclusters appear to have collapsed inwards leaving behind volumes of cooler gas. In other places, collisions between subclusters have compressed and heated the ICM. The existence of these structures within the ICM suggests that many clusters are still in the process of evolving and have not yet reached an equilibrium state.

Although such observations show that mergers do occur, it is a much more difficult task to show that mergers have played an important role in the evolution of clusters. It might at first sight appear that all that is required is to look at the relative populations of clusters at different distances.

■ Observing galaxies at great distances is equivalent to looking back in time. If the model of very rich clusters forming from the merger of smaller ones were correct, what would you expect to see when looking at clusters at greater and greater redshifts (and hence at earlier times)?

❑ You would expect to see that at high redshifts there was a greater proportion of sparse clusters (those with few members) and relatively fewer rich clusters. Over time clusters would merge, so the population of clusters with lower redshifts as seen from Earth would contain a progressively higher proportion of rich clusters.

The range and coverage of galaxy surveys continues to expand, but the population of very distant clusters has not yet been surveyed fully enough to provide a definite answer to this question: instead we must look for indirect evidence of cluster evolution.

You may recall one such piece of evidence – the *Butcher–Oemler effect* – from Section 2.5.3: out to redshifts of $z \approx 0.3$, clusters mostly look the same. More distant clusters seen at less than two-thirds of their present age have higher proportions of young blue galaxies. Many of these galaxies are deformed, probably as a result of interactions with their neighbours. This suggests a more violent past in which the galaxies within clusters were interacting with each other more vigorously than they are now, triggering bursts of star formation. This could certainly have been the case if smaller clusters were merging to form larger ones. Although rather indirect evidence, the Butcher–Oemler effect is at least consistent with the picture of clusters growing by mergers.

So, at present it seems plausible that clusters are formed by hierarchical growth, but the observational evidence to support such a claim is not strong. We will return to the formation of structure in the Universe in Chapter 6, where the role of dark matter in the formation of structure will also be examined. For now, we shall continue by looking at the problem of surveying structures larger than clusters.

4.4 The large-scale distribution of galaxies

Clusters of galaxies, with typical radii of 2 Mpc, are very much smaller than the overall scale of the Universe. As shown by Abell's survey (Figure 4.5), the distribution of clusters across the sky is not uniform – other surveys since the 1950s have confirmed this finding: clusters are not the largest scale objects in the Universe but are themselves organized into larger structures.

Much of this section will be concerned with the techniques that are currently being employed to map out the Universe on scales of hundreds of megaparsecs. However, before starting this discussion it is useful to take a quick tour of our 'local' part of the Universe beyond the Local Group.

Our Galaxy and the Local Group are part of a much larger structure: a **supercluster** – in this case, called rather unimaginatively, the **Local Supercluster** (Figure 4.17). This supercluster is centred on the Virgo cluster (Figure 4.3b), and is approximately 30 Mpc across. As suggested by Figure 4.17, this supercluster is a much more loosely organized structure than the individual clusters. Based on

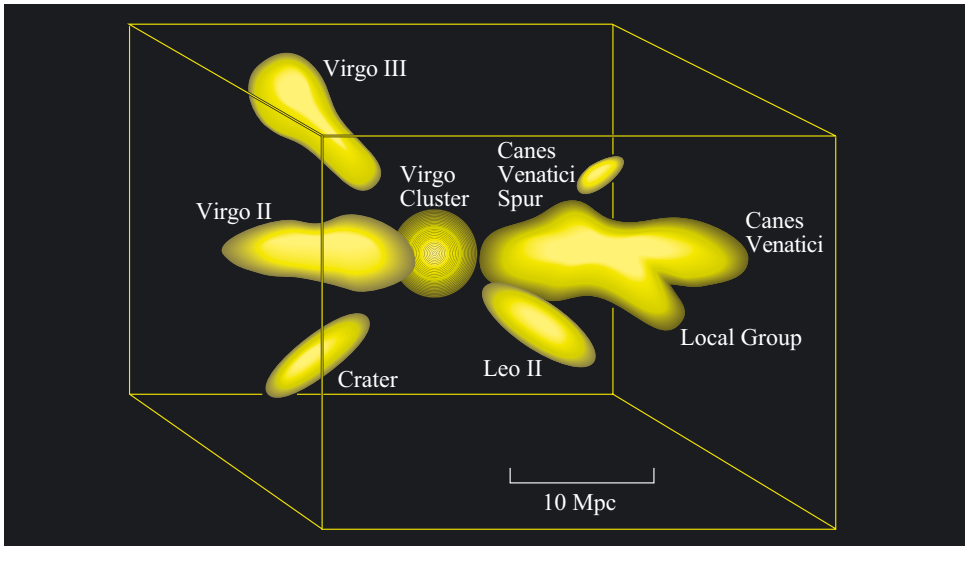

Figure 4.17 The Local Supercluster represented by a surface which separates high-density regions from lower density regions in the Universe, hence the 'empty' regions in this diagram correspond to locations were the density of galaxies is low but not zero. (R. Brent Tully)

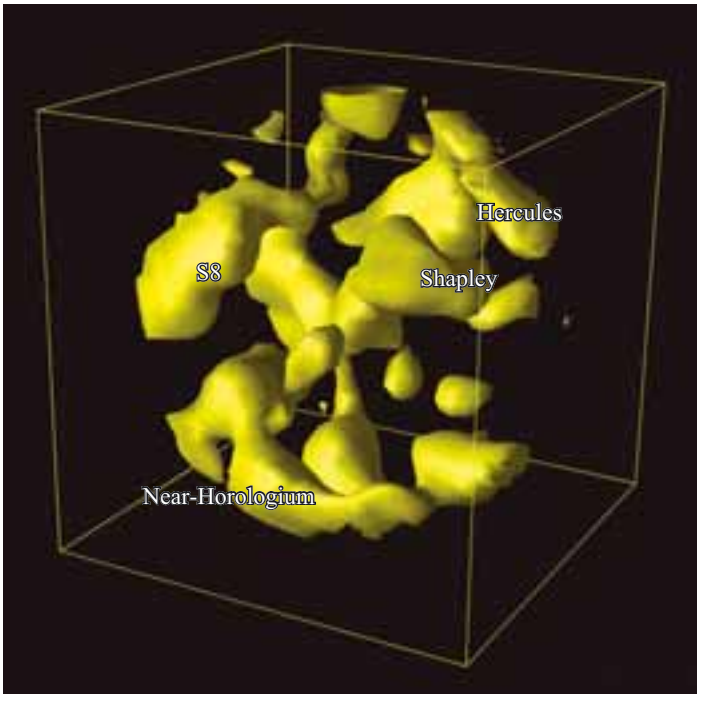

Figure 4.18 The results of a survey called PSC*z* (PSC – Point Source Catalog of the IRAS satellite, *z* – redshift) which mapped the density distribution in the Universe around us to a distance of about 250 Mpc. The locations of four superclusters are indicated: Shapley, Hercules, S8 and Horologium. Note that as in Figure 4.17, the distribution of matter is represented by a surface that separates high- from low-density regions. Also as in Figure 4.17, the 'empty' regions in this diagram correspond to locations were the density of galaxies is low but not zero. (Figure by L. Teodoro, based on data described in Saunders *et al*., 2000)

velocity measurements of the galaxies making it up, the Local Supercluster appears not to be gravitationally bound in same way that clusters of galaxies are bound, and is certainly not a virialized system.

The Local Supercluster is not unique: other superclusters in our vicinity have also been mapped. Figure 4.18 shows the results of a three-dimensional survey which mapped the volume of space with a radius of about 250 Mpc from our location. This map clearly shows the location of some nearby superclusters – with typical extents of a few tens of megaparsecs.

Since there appears to be structure on the scale of superclusters, the obvious question is whether this organization continues hierarchically to larger and larger structures. It seems that this isn't the case. Moving upwards in distance scale, recent surveys are finding that superclusters are not themselves organized into ever larger clusters of superclusters, but instead are distributed in a vast network consisting of high-density regions connected by filaments and sheets wrapped around (relatively) empty **voids**. Any structure that is on the scale of superclusters or above is often referred to by the generic term of **large-scale structure**.

An impression of the large-scale distribution of matter in the Universe can be obtained from a remarkable map (Figure 4.19) of galaxy positions that was generated by automated scanning of plates from a Schmidt telescope survey. This map was developed by a group of astronomers using the Automatic Plate Measuring (APM) facility at the University of Cambridge from plates taken at the Anglo-Australian Observatory. Although it is a two-dimensional map, the filamentary structure of the distribution of galaxies is evident.

In the next section we shall discuss how this large-scale distribution is currently being surveyed so that we can better understand the structures in the Universe around us.

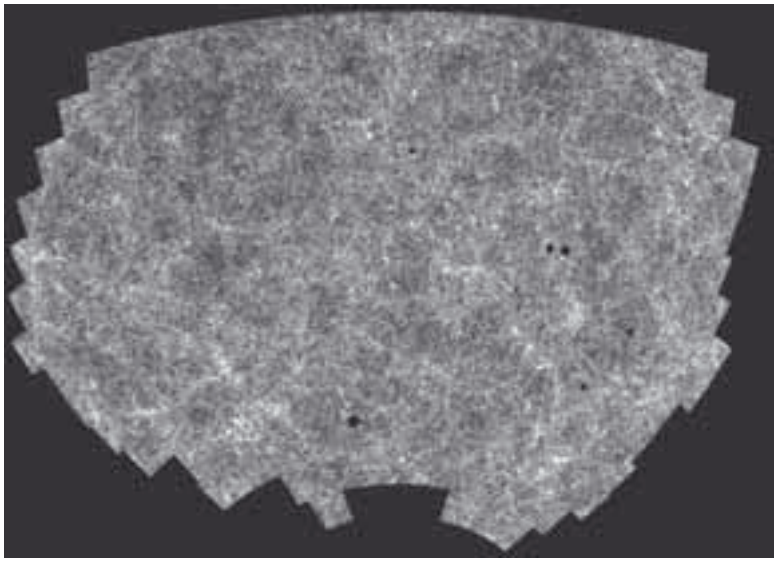

Figure 4.19 The APM map of galaxy positions. The map was generated by using automated routines to find galaxies on photographic plates. The survey contains about two million galaxies and covers an area of the southern sky that is about 4000 square degrees in extent. Note that the gaps in the map are areas that could not be scanned because of the presence of bright stars. Structure in the large-scale distribution of matter in the Universe is clearly evident in this map. (S. Maddox, W. Sutherland, G. Efstathiou and J. Loveday)

4.4.1 Redshifts of galaxies

The APM map (Figure 4.19) shows the distribution of galaxies or clusters of galaxies as a two-dimensional projection onto the celestial sphere. A comparison with constellations is appropriate here: as you may recall, the constellations do not generally represent physical groupings of stars: individual stars within a constellation may be at greatly differing distances from the Earth. Similarly, it is possible that the increased concentrations of galaxies seen in photographic surveys could be the result of coincidental alignments of galaxies at greatly different distances that just happened to be aligned along the same line of sight.

- How would you confirm that the galaxies that appear on a photographic plate to be within a cluster are indeed physically associated with each other, and not merely grouped as the result of chance alignment?

- You would need to show that the galaxies are all at a similar distance from the Earth.

This could be done by measuring the *redshift* of each individual galaxy within the cluster. If the galaxies are genuinely associated they should all have similar values of redshift. Foreground and background galaxies could be identified and eliminated by having either smaller or greater redshifts than those in the cluster. Historically, this was a difficult task due to the vast number of galaxies that had to be observed to build up a three-dimensional picture of the Universe around us. At the time that Abell carried out his initial work on clusters in the 1950s the spectra of galaxies had to be measured one at a time using a large telescope and recorded using photographic film.

Thanks to improvements in detector technology, modern telescope and detector systems can measure redshifts much more quickly. A dedicated programme of such observations can, in a matter of years, measure tens or hundreds of thousands of redshifts. Such surveys provide a basis for mapping the Universe in three dimensions. Some of the major programmes for mapping the Universe will be discussed in more detail in the following section, but first we need to take a closer look at how redshifts are related to distance.

The simple relationship $z = (H_0/c)d$ between redshift and distance introduced in Chapter 2 (Equation 2.12) is really only valid for small redshifts of up to $z \approx 0.2$: at larger redshifts this relationship no longer holds. As noted in Chapter 2, the redshift is a measure of the amount that the Universe has expanded since the light was emitted. At large distances the redshift increases more rapidly with distance than implied by Equation 2.12. For example an object with a redshift of 2.0 is not believed to be twice as far away as an object with redshift of 1.0.

There is little doubt that distance increases with redshift, but the exact relationship depends on a number of factors (or cosmological parameters) that characterize the behaviour of the expansion of the Universe. Different models of the cosmological expansion, and their consequences, will be discussed in more detail in Chapter 5. For now, it is sufficient to note that the precise relationship between redshift and distance depends on the model of the expansion used. The graph shown in Figure 4.20 represents one possible relationship between redshift and distance and will be used for the remainder of this chapter.

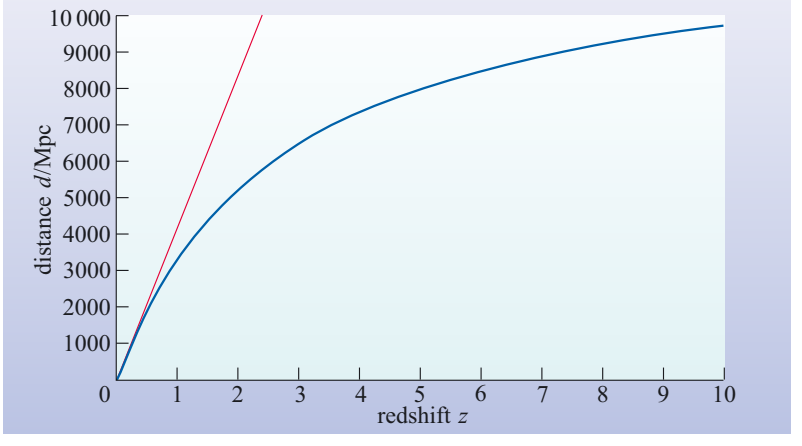

Figure 4.20 Redshift–distance relationship (blue curve) for one possible cosmological model. The simple relationship $z = (H_0/c)d$ (Equation 2.12), as indicated by the straight line (in red) holds only for low redshifts (below $z \approx 0.2$). For large redshifts, z is not proportional to distance.

4.4.2 Mapping the Universe in three dimensions

The surveys discussed in this section aim to provide accurate distance information by measuring redshifts of large numbers of objects – and some are also able to probe out to much greater distances by imaging fainter galaxies. In order to understand the scope of these surveys, we start by looking at some of the most distant galaxies imaged by the Hubble Space Telescope, such as those seen in the background of Figure 4.21.

Like the Hubble Deep Field images seen in Chapter 2, the background of this image of Abell 1689 illustrates the main difficulty with deep surveys: there are simply a huge number of very distant galaxies. The tiny portion of sky shown in Figure 4.21 contains thousands of galaxies yet the extent of the image is only 3 arcmin – one-tenth the diameter of the full moon.

■ The full moon is half a degree, or 30 arcmin, in diameter. How many images of 3 arc minutes square would be needed to survey a square area of sky 30 arcmin on a side (just large enough to cover the full moon)?

❑ You would need to assemble a mosaic of 10 × 10 images – a total of one hundred images to cover this small area of sky.

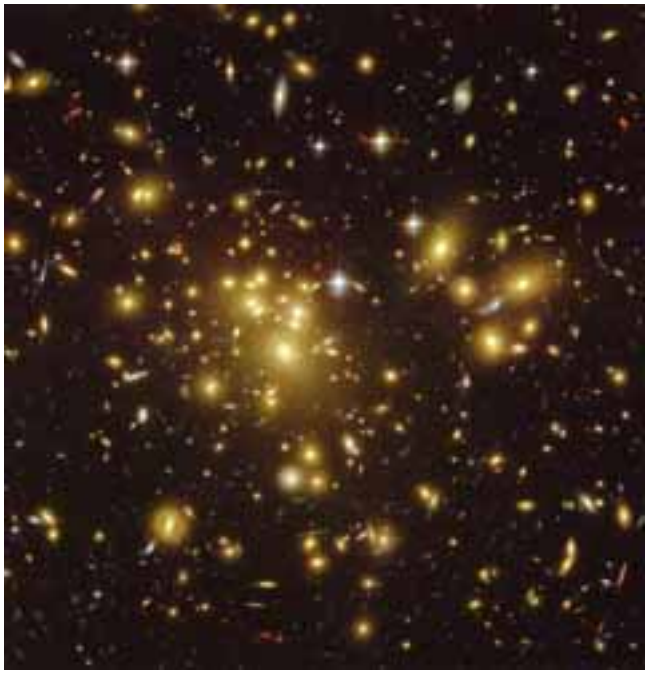

Figure 4.21 An image of the cluster Abell 1689 taken with the Advanced Camera for Surveys (ACS) on the Hubble Space Telescope. Although spectacular in its own right, the foreground cluster is overshadowed by the large number of distant galaxies that can be seen in the background. (NASA, N. Benitez (JHU), T. Broadhurst (Racah Institute of Physics/The Hebrew University), H. Ford (JHU), M. Clampin (STScI), G. Hartig (STScI), G. Illingworth (UCO/Lick Observatory), ACS Science Team and ESA)

A square image large enough to contain the full moon would be just half a degree on each side, giving an area of one-quarter of a square degree. In total there are approximately 40 000 square degrees in the whole sky. It is estimated that each square degree of sky may contain as many as 10^5 galaxies that could be detected in a long observation with the Hubble Space Telescope. Thus the total number of galaxies that we could potentially observe across the whole sky is in excess of a thousand million! Surveying the entire sky using the Hubble Space Telescope is clearly totally impractical – it would require making over ten million 3 arcmin square images.

The practical difficulties simply of imaging large numbers of galaxies are immense, but measuring their distances represents an even greater problem. Many of the galaxies imaged in the Hubble Deep Field are too faint for their redshifts to be determined. The practical constraint on the number of galaxies that can be studied in a reasonable length of time places a limit on the total volume of space that can be surveyed. Redshift surveys necessarily have had to compromise between sky coverage and distance probed: until recently it has been necessary to choose between imaging large areas of the sky to small redshifts, or small areas of sky to great distances.

Surveys carried out in the 1980s and 1990s followed one of these two paths. Some – such as the Harvard–Smithsonian Center for Astrophysics (CfA) survey (Figure 4.22a) and the IRAS (Infrared Astronomical Telescope) Point Source Catalogue *z*-survey (PSC*z* – Figure 4.18) – concentrated on measuring distances to galaxies within large volumes of the local Universe out to about 200 Mpc. Astronomers at Durham University and the University of California in Santa Cruz took a different approach, probing to much greater distances by concentrating on two much narrower regions of the sky. This **borehole survey** extended to about 2000 Mpc but covered only two narrow windows aimed towards the north and south galactic poles (Figure 4.22b).

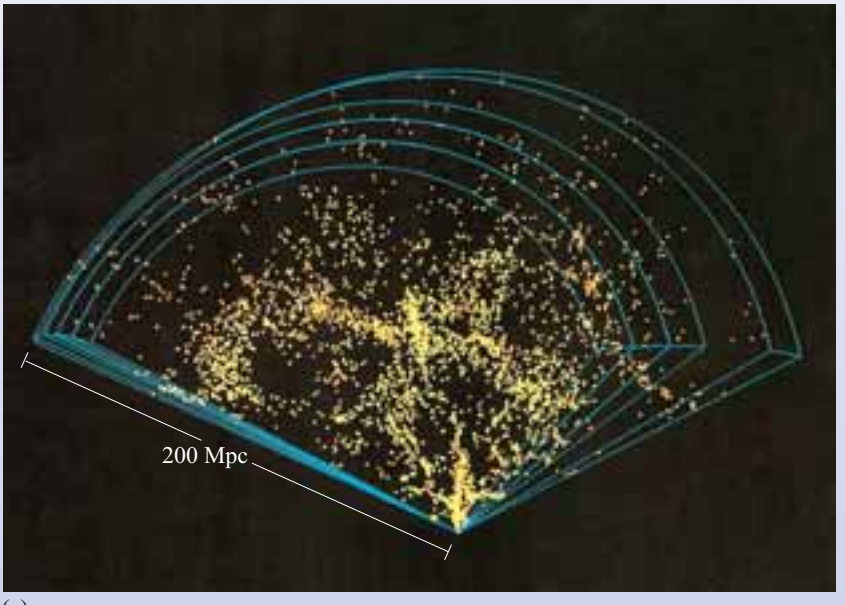

(a)

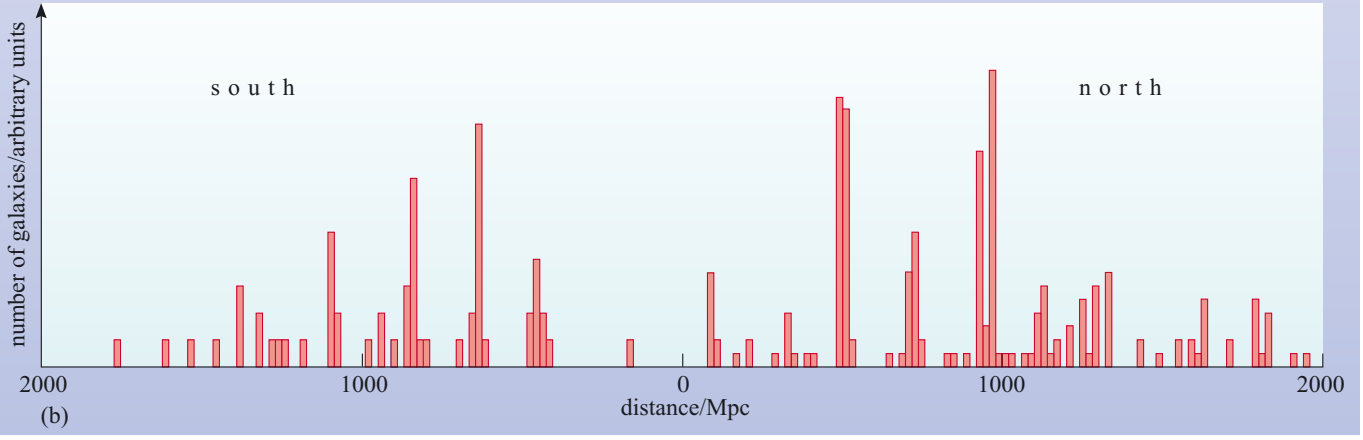

(b)

Figure 4.22 Examples of the structures revealed by the (a) CfA survey, and (b) the Durham–Santa Cruz borehole survey. Note the different distance scales. The CfA survey suggests a sponge-like distribution of galaxies with voids up to 60 Mpc across surrounded by walls and filaments. Although essentially a one-dimensional study, the Durham–Santa Cruz results also suggest the presence of walls separated by voids of low galaxy density. ((a) M. Geller and J. Huchra, SAO; (b) figure supplied by R. Ellis based on data described in Broadhurst *et al*., 1990)

Both the local surveys and the borehole survey confirmed the existence of features on scales larger than the Local Supercluster: these do not appear to be ever larger and larger clusters of clusters, but instead suggest a structure much more like a web or a network.

However, much larger volumes, going to greater depths, are needed in order to obtain a fair representation of the Universe and to see structures on the largest scales. Recent automated surveys using large-aperture telescopes are greatly extending the coverage of the sky. By contrast with the narrow views of the Hubble Deep Field, these telescopes observe with large fields of view (about 2 to 3 square degrees) allowing large areas of sky to be surveyed in a relatively short time.

The most ambitious of these projects is the Sloan Digital Sky Survey (SDSS), based at the Apache Point Observatory in the Sacramento Mountains of New Mexico (Figure 4.23). The goal of the Sloan Survey is to image one-half of the northern celestial hemisphere, as well as a smaller portion of the southern sky (see Figure 4.24). The northern sector covers roughly the same portion of the sky as Abell's 1958 cluster survey, but to a much greater depth and includes redshift

Figure 4.23 The 2.5-metre Sloan telescope has a remarkably wide-angle field of view, and is designed specifically to create a map of the sky. The telescope's detector includes an imaging camera and two spectrographs. The boxy metal structure that is prominent in this photograph is the outer wind baffle, which helps to minimize vibration of the telescope. (Sloan Digital Sky Survey)

measurements as well as simply imaging the galaxies. The aim is to determine the positions and brightness of over 100 million objects including stars, quasars and galaxies. By measuring the redshifts of a million of the nearest galaxies the survey will provide a three-dimensional picture of our neighbourhood of the Universe.

The survey has two elements: a deep sky imaging survey and a spectroscopic survey to determine redshifts. The imaging survey will record objects as faint as an apparent magnitude of 24. From these 100 million objects, the brighter ones (apparent magnitude 19 or brighter) will be selected for redshift measurements – this will include over a million galaxies and quasars. Hence only a small fraction of the objects imaged by SDSS will have their redshifts measured. It is expected that typical galaxies will be measured up to a redshift of about 0.25. The observational phase of the programme, which began in 2000, is due to be completed by 2005.

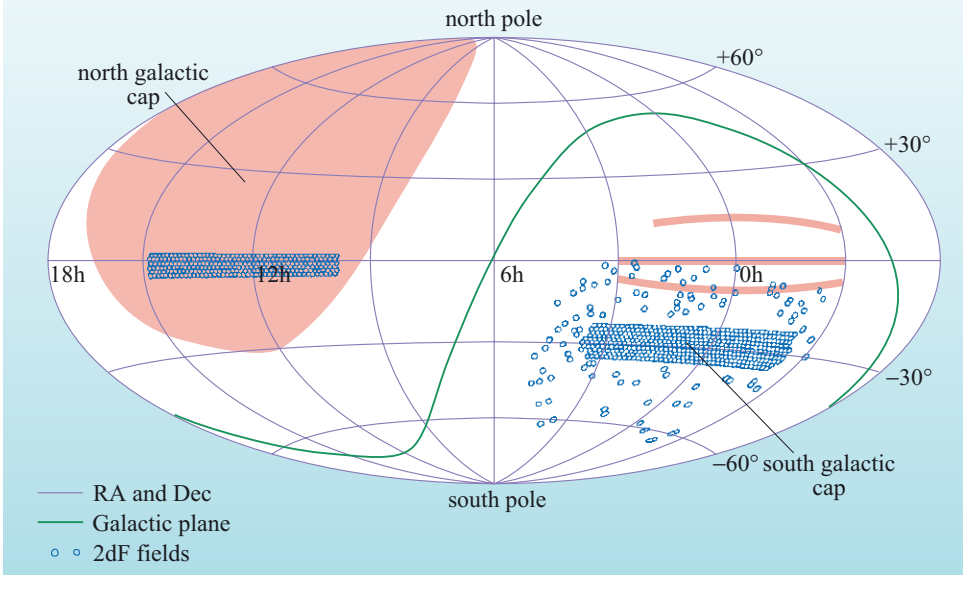

Figure 4.24 A map of the entire sky in equatorial coordinates showing the survey regions of the SDSS survey (pink shading), and the 2-degree Field (2dF) survey (blue shading). (Prepared with the assistance of M. Colless, Mount Stomlo Observatory)

The SDSS will cover most of the northern sky above 30° north of the galactic plane. Within this area it will generate a detailed three-dimensional map of our local neighbourhood out to ~800 Mpc, and a (two-dimensional) imaging survey out to much larger distances.

Another major redshift survey, albeit on a smaller scale than the SDSS, is the 2-degree Field (2dF) survey. This project, which had an observational programme that lasted three years (completed in 2002) was carried out using the 3.9 metre Anglo-Australian Telescope. Using a camera with a two-degree field of view, it surveyed two wedge shaped sectors of sky, one to the north and one the south of the galactic plane as shown in Figure 4.24. One aim of the survey was to use galaxy redshifts and positions to map the structure of the Universe out to distances of about 600 Mpc (this is the 2dF Galaxy Redshift Survey – 2dFGRS). The 2dF survey also mapped quasar positions and redshifts to much greater distances. Although the observational phase of the 2dFGRS is now complete, the analysis of the data will continue for many years.

The SDSS and the 2-degree Field survey use optical fibre systems to collect the spectra of hundreds of galaxies simultaneously. This means that the redshift measurements from many galaxies in a single field-of-view can be collected at the same time. Compared to older techniques in which only one spectrum could be measured at a time, modern fibre optic systems give a great advantage in the rate at which data can be collected.

In addition to surveying galaxies, both projects will also record the distances to hundreds of thousands of quasars and this will extend both our knowledge of the distribution of matter at high redshifts and provide information about the evolution of active galaxies (Section 3.6.2).

The improvements in imaging sensor technology over the past few decades are enabling these wide-scale surveys to be carried out in far more detail than was possible before, even using telescopes with relatively small apertures. When the same imaging technology is coupled to a large telescope, surveys can be extended to very high redshifts.

A group led by the University of California in Santa Cruz is doing exactly that in a project involving two of the most powerful telescope systems available. This Deep Extragalactic Evolutionary Probe project (DEEP) is using the twin Keck 10-metre telescopes on Mauna Kea, Hawaii, and the Hubble Space Telescope, to carry out a redshift survey that will include 50 000 galaxies to a limiting magnitude of 24.5 – equivalent to a redshift of 1.55 or a distance of about 4000 Mpc.

Like the earlier borehole survey, DEEP will cover only a very small area of sky, but will go out to much larger redshifts than the wide area surveys of the Sloan Digital Sky Survey and the 2-degree Field project. The patches of sky that will be examined include tiny portions of the area surveyed by SDSS and the area imaged in the original Hubble Deep Field. DEEP is designed to study the distribution and the evolution of galaxies out to high redshifts, thus exploring conditions earlier in the history of the Universe.

A summary of important redshift surveys that are either ongoing or have been completed is given in Table 4.2. Figure 4.25 shows the coverage in terms of area of sky and distance of these different surveys.

Table 4.2 A summary of five important galaxy redshift surveys. The CfA and the PSC*z* surveys were completed in 1989 and 1997 respectively.

Name	Number of galaxies in survey (approximate)	Mean redshift	Telescope diameter/m	Simultaneous spectral measurements[a]
CfA	1500	0.02	1.5	1
PSC*z*	15000	0.03	2.1	1
2dFGRS	250 000	0.10	3.9	400
SDSS	1000 000	0.10	2.5	640
DEEP	50 000	0.7–1.55	10	1

[a]The number of simultaneous spectral measurements describes how many galaxy redshifts can be measured in a single field-of-view at any one time.

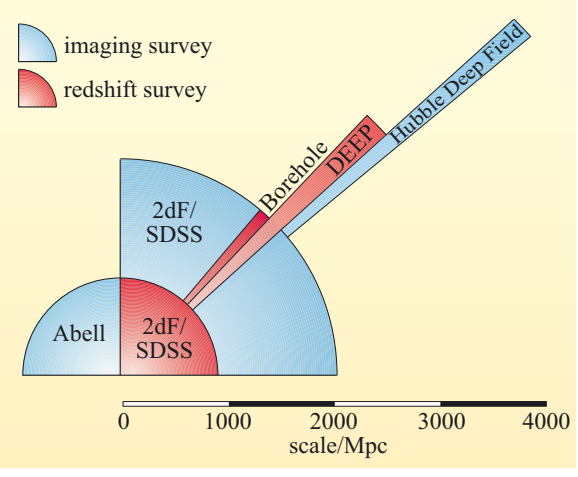

Figure 4.25 A schematic illustration of the relative scales of the different surveys. Imaging surveys can include fainter objects than redshift surveys, so the imaging elements of the SDSS and 2dF projects go out to much greater distances than their corresponding redshift elements. (Note that the extent of the sectors in this diagram are for illustration only – they do not correspond to the actual areas of sky covered by these surveys.)

4.4.3 Large-scale structure revealed

Although several of the surveys discussed in the previous section are still ongoing, early data releases are revealing ever larger glimpses of the structure of the Universe. One example is the result from the 2-degree Field survey shown in Figure 4.26.

The 2dF results clearly show that the web or sponge-like structure suggested by earlier studies extends out to great distances, forming a cosmic network. The densest points within this network are clusters of galaxies containing hundreds or thousands of galaxies. Loose collections of clusters form superclusters of perhaps 30 to 50 Mpc in size. On larger scales, there are low-density voids, of up to about 60 Mpc in diameter, separating the higher density collections of clusters. These voids are separated by filaments of galaxies strung out in long chains, and by two-dimensional sheets that enclose the voids rather like the pores in a sponge. Although difficult to discern from representations such as Figure 4.26, the density of galaxies in the filaments is very much less than that in the clusters, and only a factor of two or three greater than the density in the voids themselves. The largest structures appear to be on a scale of approximately 200 Mpc; above this, the Universe becomes uniform in the sense that one 200 Mpc region looks much like another.

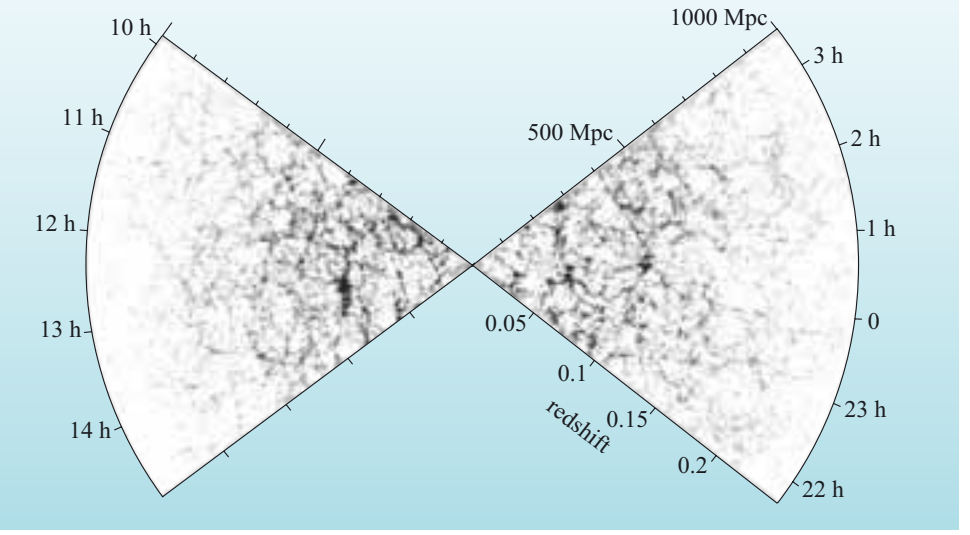

Figure 4.26 Early results from the 2-degree Field Galaxy Redshift Survey. This data release (May 2002) shows the positions of over 220 000 galaxies plotted in plan view on the two wedges covered by the survey. (M. Colless, Mount Stomlo Observatory)

QUESTION 4.5

Summarize the scales of different cosmic structures by completing Table 4.3. Note that only approximate values, or ranges of values, are required.

Table 4.3 The scales of different types of cosmic structures – for use with Question 4.5.

Feature	Distance or length/Mpc
Milky Way (diameter of the stellar disc)	
Distance to Large Magellanic Cloud	
Distance to the Andromeda Galaxy	
Extent of the Local Group	
Typical diameter of a cluster	
Distance to nearest rich cluster (Virgo)	
Extent of a typical supercluster	
Extent of voids	
Scale on which the Universe appears uniform	

4.5 The spatial distribution of intergalactic gas and dark matter

In the case of clusters of galaxies we saw that the galaxies themselves make only a small contribution to the total mass: clusters also contain significant amounts of intracluster gas, and the total mass is dominated by the contribution from dark matter. We also saw that in clusters the intergalactic gas and the dark matter are distributed in a somewhat different way from the galaxies. Specifically, the dark matter and the intergalactic gas seem to be more smoothly distributed in a cluster

than do the galaxies. So it is of great interest to astronomers to understand how intergalactic gas and dark matter are distributed on large scales – do they follow the large-scale structure that is mapped out by the luminous matter in galaxies, or is their distribution significantly different?

We will begin by considering how the gas that lies between galaxies and clusters can be studied, before moving on to discussing a technique that is now being developed to map the distribution of dark matter in the Universe.

4.5.1 Quasars and the Lyman α forest

We saw earlier that the intergalactic gas in clusters of galaxies is easily detectable because of its X-ray emission. However, in locations that are away from the gravitational influence of a rich cluster the intergalactic gas will not be a bright source of X-ray emission, or indeed, of any other form of electromagnetic radiation. A different type of approach is needed if we are to study such gas. Rather than looking for *emission* from this gas, astronomers examine how it *absorbs* electromagnetic radiation. Of course, to do this, there needs to be a convenient source of electromagnetic radiation that lies beyond the gas we wish to study. Fortunately, distant quasars provide us with such a source.

As you saw in Chapter 3, quasars are very bright, point-like objects with very high redshifts: quasars with redshifts up to about 6 have been discovered. Since they lie at such large distances from us, the electromagnetic radiation that is emitted by most quasars will cross vast tracts of the intergalactic medium as it travels towards the Earth. As this electromagnetic radiation passes through this medium we might expect that a certain amount of absorption may occur and give rise to spectral absorption lines at specific wavelengths (Figure 4.27).

The most common element in the Universe is hydrogen, and the distribution of intergalactic gas can be mapped by making use of the spectrum of this element. The spectrum of hydrogen consists of several series of spectral lines. Of these, the **Lyman series** has the highest energy (and hence shortest wavelengths). Within this series, the most prominent spectral line is the Lyman α line corresponding to the transition between $n = 2$ and $n = 1$ levels of the hydrogen atom. This line, which is often abbreviated to Lyα, lies in the ultraviolet part of the spectrum with a wavelength of 121 nm and is easily identified, even when red-shifted.

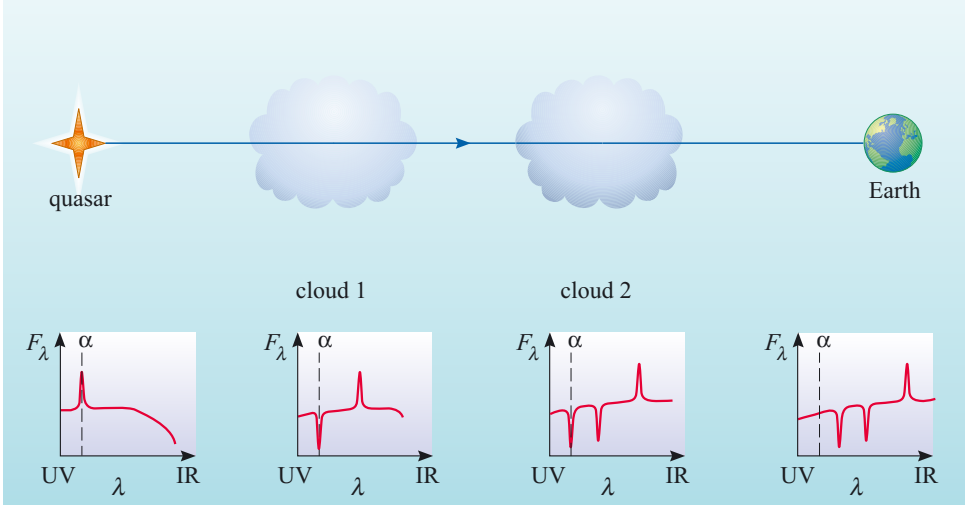

Figure 4.27 Intervening clouds in the line of sight from a quasar. Cloud 2 will have the smallest redshift when viewed from Earth.

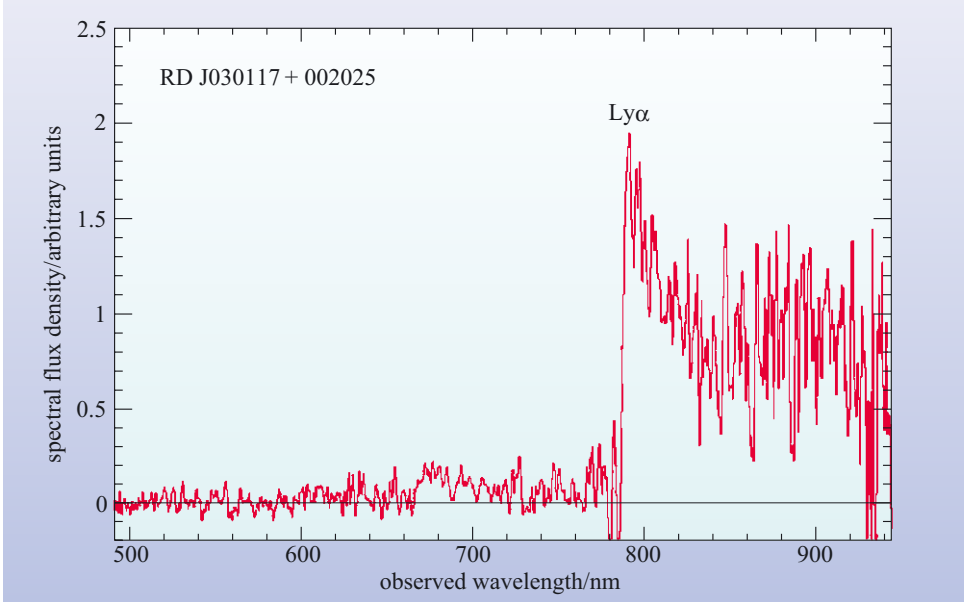

Figure 4.28 The spectrum of quasar RD J030117 + 002025 with redshift of $z = 5.5$. The redshift of this object is so large that the Lyman α emission line has been shifted from the ultraviolet (121 nm) to the infrared (786 nm). (Stern *et al.*, 2000)

In the spectra of the most distant quasars the Lyman α spectral line gets shifted all the way from the ultraviolet, through the visible part of the spectrum and into the infrared (Figure 4.28). In the original spectrum from the quasar, this line is present as a bright *emission* line, which appears above the continuous spectrum produced by the AGN (see Figure 3.16).

As the electromagnetic radiation from the quasar passes through intergalactic space it encounters clouds of cool gas. Because the gas is cool, absorption will occur, and this will be prominent at the wavelength of the Lyman α line. To an observer within one of these clouds the spectrum from the quasar will appear red-shifted, so the original Lyman α emission line will have a longer wavelength than 121 nm. Ultraviolet light that arrives at the cloud with a wavelength of 121 nm would have been emitted by the quasar at wavelengths shorter than the Lyman α line. The cloud will absorb radiation at a wavelength of 121 nm and so an absorption line will be formed. This process of absorption will occur for every cloud that the light from the quasar passes through. However, these clouds are at differing distances from the quasar, so according to observers situated on these clouds, the observed emission from the quasar will be red-shifted by differing amounts. Consequently, as the electromagnetic radiation from the quasar passes through a series of clouds on its way to Earth, it produces a set of spectral lines at progressively shorter wavelengths. The distances to the clouds can be found from the redshifts of these absoption lines. An example of a spectrum from the quasar Q 0149+336 which displays such absorption features is shown in Figure 4.29.

Because of the many closely packed absorption lines, this structure in a spectrum is frequently referred to as the **Lyman α forest**.

- What does the presence of discrete absorption lines in the Lyman α forest suggest about the distribution of the material that the light has passed through? What would be seen if the absorbing material were distributed *uniformly* along the line of sight?

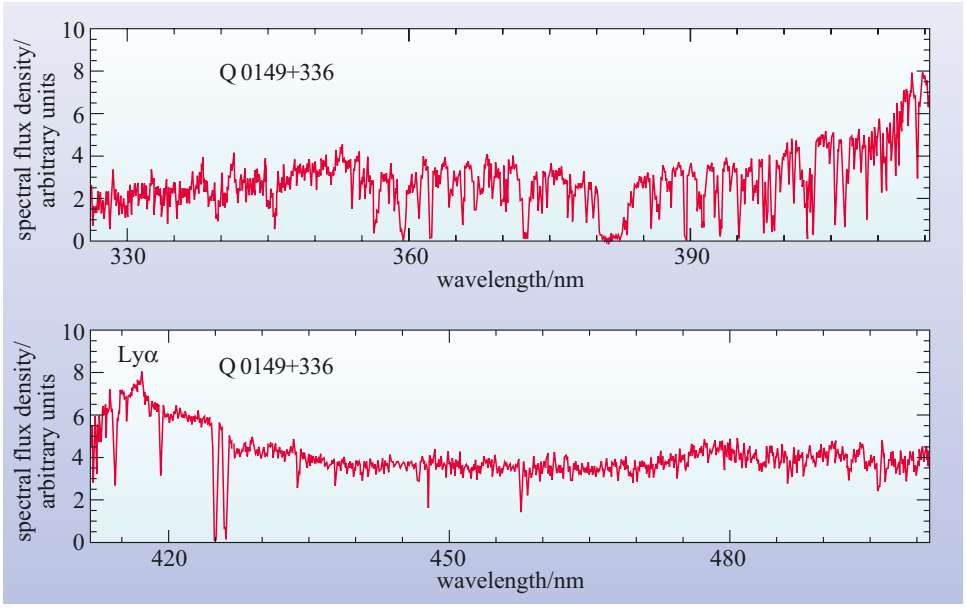

Figure 4.29 The spectrum of quasar Q 0149+336 ($z = 2.431$). The upper panel shows the spectrum from a wavelength of about 325 nm to 415 nm, the lower panel shows wavelengths from about 410 nm to 500 nm. The red-shifted Lyα line has an observed wavelength of 417 nm. At wavelengths shorter than the (red-shifted) Lyα line, there are a large number of absorption lines – due mainly to Lyα absorption by clouds of intergalactic gas at lower redshift than that of the quasar. At wavelengths longer than the red-shifted Lyα line there are relatively few absorption lines (the lines that are present are not due to Lyα absorption, but to absorption by elements heavier than hydrogen or helium in the intergalactic medium). (Wolfe *et al*., 1993)

❑ In order to produce a distinct absorption line at a given wavelength, the light must have passed through a concentration of material at the distance corresponding to that redshift. If the material were distributed uniformly, light would be absorbed gradually all along the line of sight with continuously varying redshift, giving constant absorption at all wavelengths rather than a 'forest' of individual lines.

So the fact that there are many Lyman α absorption lines in the spectrum from a distant quasar tells us that the intergalactic medium is not smoothly distributed – but instead is in the form of 'clumps' or clouds.

For example, an analysis of the absorption lines in the spectrum of the quasar Q 0149+336 (Figure 4.29) reveals seven clouds along the line of sight whose presence is confirmed by absorption lines due to elements heavier than hydrogen or helium ('metals'). Each of these clouds has a distinct redshift (ranging from about 0.5 to about 2.2 in this case). Note that there are many other lines, which are also due to absorption by intervening clouds, but that it is not possible to confirm the presence of any single cloud unless a *pattern* of spectral lines (Lyα and metal absorption lines) can be discerned in the spectrum.

QUESTION 4.6

In Figure 4.29, the spectrum shows a strong absorption line at a wavelength of 372 nm. Assuming this to be a red-shifted Lyman α line, calculate the redshift and hence estimate the distance of the cloud responsible for this absorption line.

So how does this distribution of intergalactic gas correspond to the distribution of matter as traced by galaxies? This is an ongoing area of research, but it does seem as though the Lyman α absorbing clouds are more uniformly distributed in space than the luminous matter. For instance, it has been mentioned that there are 'empty-

spaces' or voids in the galaxy distribution, but clouds of absorbing gas do seem to be present in these voids. There is no inconsistency here: most Lyman α absorbing clouds have very low densities – too low to be sites of star, and hence, galaxy formation, so it need not be the case that the distribution of intergalactic gas should exactly follow the distribution of galaxies.

Although the majority of Lyman α absorbing clouds are of low density, there are some clouds where the density enhancement is about a factor of 10^6 above the mean density of the intergalactic medium. The absorption lines from these clouds are very deep and broad, and are called **damped Lyman α systems** (the terminology 'damped' refers to the physical effect that gives these lines their characteristic shape). The trough at roughly 380 nm in Figure 4.29 is an example of this effect. Damped Lyman α systems are of particular interest because, unlike the low-density Lyman α clouds, they *are* a plausible source of material for star formation. Indeed, it is suspected that the damped Lyman α systems may be clouds from which galaxies are about to, or have started to form. Unfortunately the evidence to make such a connection is, at present, rather circumstantial, but clearly these systems will be subject to a great deal of scrutiny in the coming years.

The fact that radiation from a distant quasar can reach us at all appears at first sight surprising. In Chapter 2, we saw that the big bang model suggests a Universe that is initially filled with a smooth distribution of hydrogen and helium which cools and forms neutral atoms. This is then followed by the growth of density perturbations by gravitational collapse. The matter that does not take part in this process might be expected to remain as un-ionized gas. The quantity of neutral gas that might naively be expected to remain in the intergalactic medium is such that it would cause very strong absorption of the light from distant quasars. This expected absorption by a neutral intergalactic medium is called the **Gunn–Peterson effect**. The fact that the absorption, as seen through the Lyman α forest, is much lower than expected suggests one of two possibilities: either that the expected hydrogen is not present, or (more likely) that any hydrogen is present but not as neutral hydrogen, rather it is in an *ionized* state, that prevents it from absorbing the radiation.

For light to reach us from distant quasars, intergalactic hydrogen must have been ionized by the time the light was emitted. The event that caused most of the neutral hydrogen in the Universe to become ionized is referred to as **reionization**. The time at which this occurred is called the **epoch of reionization**, and to be consistent with observations of high-redshift quasars this must have been when the Universe was less than 10% of its current age. So what could have caused this Universe-wide change? The most plausible explanation is that sources of ultraviolet radiation suddenly 'turned on' at this time.

■ Can you suggest two possible sources for this ultraviolet radiation?

❑ Star-forming regions and active galactic nuclei are both strong sources of ultraviolet radiation.

As we saw in Section 2.5.5, galaxies seen at high redshifts appear to be sites of energetic bursts of star formation. This was happening when the Universe was only about 10% of its present age, and could have provided the energy required to ionize the intergalactic hydrogen. Alternatively, you saw in Section 3.6.2 that in the past the density of quasars was much higher than it is now. So it is also possible that

active galaxies provided a source of ultraviolet radiation that ionized the bulk of the neutral hydrogen in the Universe. At present there is no consensus about which of these two processes was the more important as a cause of ionization of the neutral intergalactic medium.

If it were possible to look back to times earlier than the epoch of reionization, then we should expect quasar spectra to show strong absorption from neutral hydrogen. The search for the Gunn–Peterson effect at these early epochs is currently an active area of research. Recent observations of the most distant quasars are beginning to show signs that the expected absorption has indeed been detected at redshifts greater than $z \sim 6$. If confirmed, these results will allow estimates to be made of the time in the early Universe at which stars or active galaxies first started to form.

4.5.2 Cosmic shear

All the methods of determining masses discussed in Section 4.4 point to the existence of dark matter within galaxies and clusters. A fundamental question is whether the large-scale distribution of galaxies follows the distribution of dark matter as suggested by theoretical models. In many of these models, dark matter condenses first, creating a network within which galaxies form at locations where the dark matter is most densely concentrated.

Dark matter cannot be observed directly because it does not absorb or emit light. Within galaxies and clusters its presence can be detected by its gravitational effects on the velocities of individual stars or galaxies. Superclusters and larger structures however are not virialized so the large-scale distribution of dark matter cannot be studied in the same way.

■ Can you think of another way in which dark matter might reveal its presence on a large scale?

❑ Dark matter does not emit or absorb light, but it can be detected by its *gravitational* effects on light. The large-scale distribution of dark matter could be studied by looking for deflections of light from distant galaxies.

A strong form of gravitational lensing was seen in Section 4.3.2 where large local concentrations of mass such as clusters of galaxies acted as gravitational lenses causing severe distortions of background objects. Diffuse large-scale structures can also affect the paths of light rays causing a weaker form of the effect, where fluctuations in the density of matter cause the images of background galaxies to be very slightly stretched and distorted. This effect is known as **cosmic shear** and is similar to looking at the tiled bottom of a swimming pool through the ripples on the surface (Figure 4.30).

■ What effect would dark matter have on the passage of light if it were distributed uniformly throughout the Universe?

❑ None: if the distribution of dark matter were completely smooth, the light would not be deflected one way or the other. By analogy, the bottom of swimming pool would not appear distorted if the surface were smooth – it is the ripples that cause the distortion. Only if there is a non-uniform distribution of mass would deflections be seen.

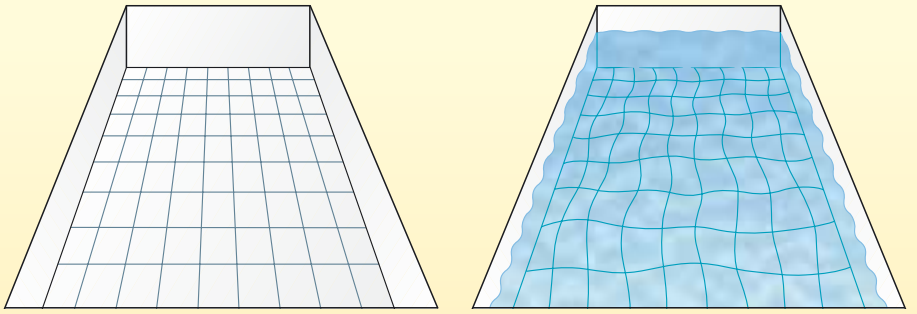

Figure 4.30 The bottom of a swimming pool can appear distorted when viewed through ripples on the surface. In a similar way, light from distant galaxies can be distorted as it passes through a non-uniform distribution of dark matter.

In the example of the swimming pool, the grid pattern of the tiles on the bottom of the pool makes even small distortions easy to see. The square tiles become distorted by the ripples on the surface: this type of distortion is known as a *shear*, hence the term *cosmic shear*. The sky, of course, does not have a convenient grid painted on it! Instead, use can be made of very distant galaxies such as those seen in long-exposure observations made using the Hubble Space Telescope (Figure 4.21): if you look to a great enough distance there are a vast number of background galaxies in every tiny patch of sky.

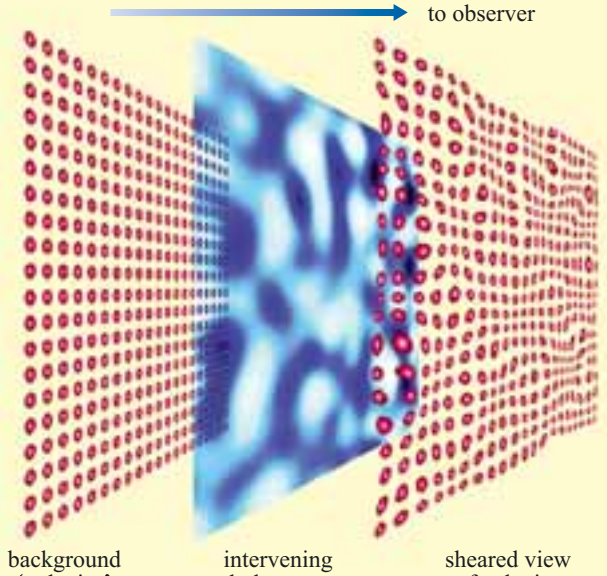

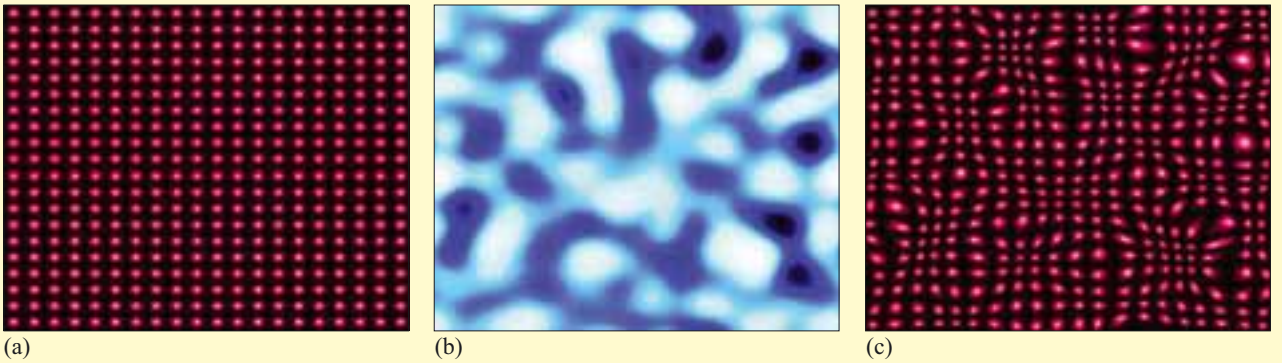

Figure 4.31 Cosmic shear: As light from a field of distant galaxies (a) passes through the web of dark matter (b) on its way to Earth, the image of each galaxy is slightly distorted by the non-uniform gravitational field (c). Although the distortion of each galaxy is small, the *average* distortion in a region of the image can be used to map the distribution of dark matter. (Adapted from figures produced by A. Refregier, University of Cambridge)

Figure 4.31 shows an imaginary situation in which a distant regular array of circular galaxies is viewed through a web of dark matter. Note how distortions indicate the presence of a high density of intervening dark matter. In other parts of the image, the 'galaxies' are relatively undistorted – showing that light rays have passed through a region with little variation in density. In reality, the distortions are much smaller – only one or two per cent, and the outlines of real galaxies are not necessarily circular to start with, so the distortion of an individual galaxy can be difficult to measure. But the images of galaxies that are near to one another will tend to be stretched in the same direction, and each small area of sky contains many galaxies. So even if the distortions are small they can still be measured by *averaging* over many neighbouring galaxies. This average distortion of galaxies can be used as a measure of the intervening dark matter.

Gravity is the one known way in which dark matter makes its presence felt. Because the distortions of background galaxies are caused by gravitational fields, cosmic shear provides one of the most direct means of mapping the distribution of dark matter.

This type of measurement is in its infancy, but the cosmic shear results published so far *do* suggest a network of dark matter that is consistent with the position of the visible matter in the Universe as mapped by redshift surveys. This is a vital piece of evidence with relevance to possible models of the formation and evolution of cosmic structure which will be taken up in more detail, in Chapter 6.

4.6 Describing cosmic structure

In this section we will introduce some of the ideas that are used to describe or characterize cosmic structure. We have already seen that the distribution of galaxies seems to suggest that at scales of about 200 Mpc or so, the Universe becomes uniform – one region that is about 200 Mpc across tends to look very much like another. However, theories of how structure is formed in the Universe need to be tested against real observations of the distribution of matter.

Computer simulations play an important role in the comparison between theory and observation. Different theoretical models make different predictions depending on the conditions built into the model. For example, changing the amount of dark matter in a computer simulation may make a large difference in the predicted distribution of galaxies. Theories can therefore be tested by varying the parameters within simulations (such as for instance, the density of dark matter) and comparing the results with data from the surveys.

It is unreasonable to expect that a computer simulation would reproduce the exact positions of all the individual galaxies in the Universe – rather, we expect theory to generate structures that are *similar* to those observed in the real Universe. For example, a good theoretical model should result in the formation of structure on scales that agree with observations – the *distribution* of galaxies should generate patterns similar in both shape and scale to those measured by redshift surveys.

The problem of describing the distribution of clusters can be tackled in various ways. As a very simplified example, look at Figure 4.32a, which shows a two-dimensional distribution of points. This could, for instance, correspond to a distribution of the positions of galaxies as seen on the sky. To describe this

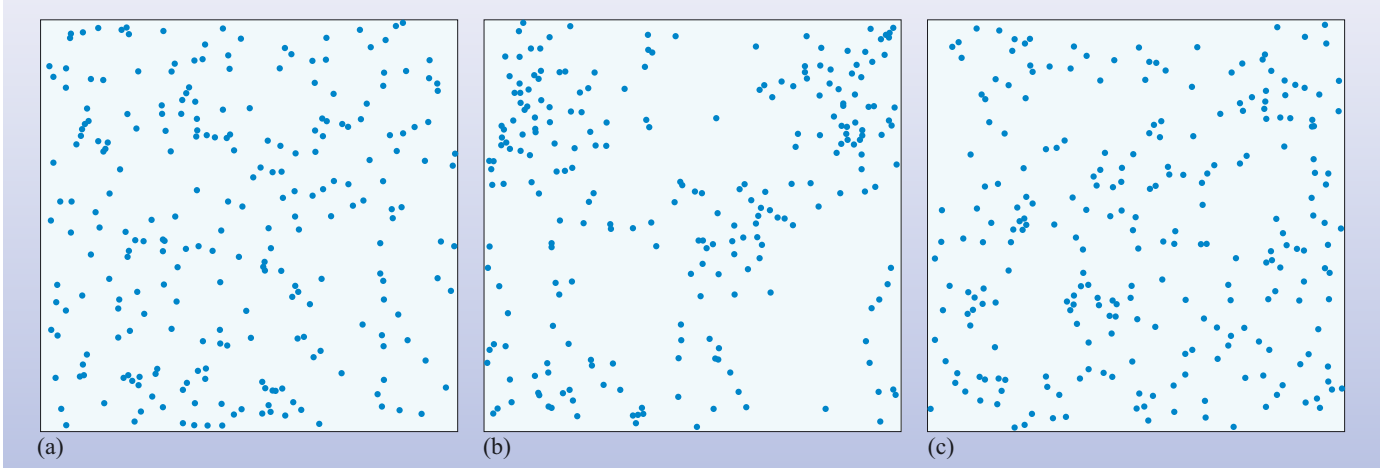

Figure 4.32 Three different two-dimensional distributions of points.

distribution the positions (for example, the x and y coordinates) could be given for each of the points. This would describe the distribution exactly, but it would not be useful to an astronomer who wants to make comparisons with a simulation. A description is needed which will easily allow comparison between different parts of the sky or between observations and simulated distributions, which will tell us how such a pattern may have formed.

The process of comparison of patterns is something that the human brain seems to be quite well adapted to do, as the following example should illustrate.

■ Look at Figure 4.32, and by eye, compare the pattern in (a) with those in (b) and (c). Which of (b) and (c) would you say most closely resembled (a)?

❑ Most people would choose (c) as being a pattern that resembles (a),

■ Why would you say that (c) more closely matches (a) than does (b)?

❑ Pattern (b) looks distinctly different. There seem to be clumps of galaxies and empty spaces that are not evident in (a) and (c).

The human brain does a remarkable job in being able to match patterns, but astronomers need a rigorous way of describing patterns which can be automated and applied to different sorts of data. To do this, astronomers use statistical methods that describe the average properties of a given distribution or pattern.

It would be a lengthy and highly mathematical diversion to explore all the various techniques that astronomers have adopted in order to compare maps of the Universe with the output from simulations. Indeed, the astronomical literature is littered with discussion about the advantages and disadvantages of using a particular statistical technique to characterize the large-scale distribution of matter in the Universe.

However, it is instructive to consider one type of method that is used, since it highlights the aim of all such techniques, which is to quantify how the relative variation in density in a map depends on length scale.

We will consider a simplified example of a technique that is called the **counts-in-cells** method. As the name suggests, the basis of the technique is to split a map (or three-dimensional survey region) up into cells and count the number of galaxies in each cell. As the following example shows, by carrying out this process using cells of differing sizes, it is possible to quantify how the density of galaxies varies on different length scales.

The maps that we will characterize in this example are two-dimensional, although the argument that we will follow can equally well be applied to three-dimensional surveys. To simplify the method, the maps are square and both have an area of 128 units by 128 units. These 'units' are our way of defining length in these maps.

Figure 4.33a (top left panel) shows the first map that we will be interested in – it shows a hypothetical distribution of galaxies all of the same mass, represented by points. In fact, this is a purely random distribution – the probability of finding a galaxy is the same at any location on the map, and we will call this distribution the 'random' map.

We are interested in investigating how fluctuations in density depend on length scale, so what we can do is to split the map up into cells and measure how the variation in density depends on the cell size. To start with we split the map up into 64×64 ($= 4096$) cells – so each cell has a size of 2 units $\times$ 2 units. In each of these cells we count the number of galaxies and hence calculate the density (remember that these are all 'galaxies' of identical mass). These densities are indicated in Figure 4.34a (top middle panel) by the shading of the cells (the brighter cells have a higher density). For all of the 4096 cells in this map we then work out a 'typical' variation $\Delta\rho$ – the amount by which the density of any one cell is likely to differ from the mean density ρ (taken over the entire map). The *relative variation* in density is then defined as $(\Delta\rho/\rho)$. In this first case, where the cell size is 2 units, the relative variation turns out to be 100%.

The next stage is to repeat this process with a smaller number of cells – in this case 32×32 ($= 1024$) (Figure 4.33a – top right panel). As you might expect, the relative variation is now smaller because the cells are larger – in fact, it is now only about 50%. This process can be repeated for cells in which the map is split up into increasingly larger cells: 16×16 ($= 256$), 8×8 ($= 64$) and 4×4 ($= 16$) cells (Figure 4.33a – second row of maps). When this is done the relative variation is found to have values of 24%, 11% and 4% respectively. As expected, the relative variation decreases as the size of the cell increases – the variation in the map is 'washed-out' as we look at the map at larger and larger scales.

The final stage is to plot a graph that shows how the relative variation changes when the map is split up into cells of different sizes. To do this a graph can be plotted of relative variation against the length of one side of the cell. For the example that we have just considered, such a graph is shown as the blue line in Figure 4.33c.

To illustrate how such a technique can provide a useful way to compare two maps, Figure 4.33b shows another hypothetical distribution of galaxies. As in the 'random' map, the map contains galaxies of identical mass, but in this case the distribution is strongly clustered. This will be referred to as the 'clustered' map. (Note that this distribution is much more clustered than the real distribution of galaxies.) Figures 4.33b show the results of applying the identical technique to that we have just described for the 'random' map to the 'clustered' map. The cores of the clusters have very high density, and this causes the relative variation to be very high (about 320%) when we analyse the map at a resolution of 64×64 cells.

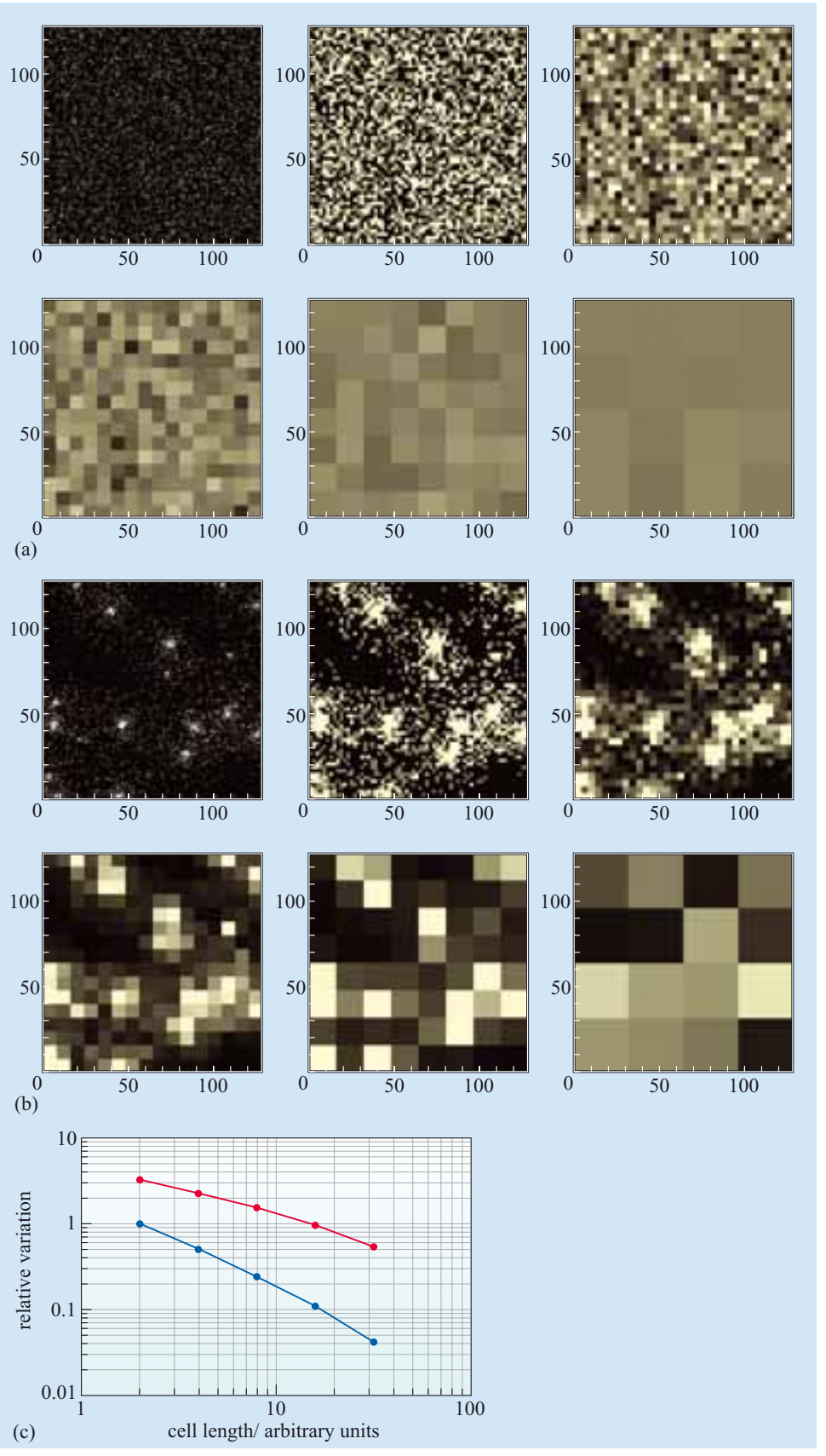

Figure 4.33 The counts-in-cells technique for measuring how the size of variations in density depend on the size of cell.
(a) Shows the original map (upper left), and five realizations of the same data binned into cells of increasingly larger sizes. The density within a cell is indicated by the intensity of its shading – brighter shading indicates higher density. The original map in this case is a purely random distribution of galaxies.
(b) Shows the same analysis as in sequence (a), but in this case for a highly clustered distribution.
(c) Shows a graph of how the relative variation depends on the size of the cell. The blue line shows the results from the 'random' map and the red line shows the results from the 'clustered' map. (M. Jones (Open University))

As cell size increases, the relative variation decreases, again because the variation is 'washed-out' in the larger cells. However, note that the clustering also causes large 'voids' and even when the map is analysed at a resolution of 4 × 4 cells, there is substantially more relative variation – typically 50% – than was found in the 'random' map.

The results of this analysis for the 'cluster' map are shown in Figure 4.33c (red line). Note that the results of the counts-in-cells analysis for the two maps are very different – not only does the cluster map show more relative variation at every length scale, but the shapes of the two curves in Figure 4.33c are also different. Of course, the technique that has been described here can be equally applied to a simulation as to real data – so by comparing the counts-in-cells analysis of real maps with simulations we may be able to discern which theoretical models for structure formation are consistent with observation.

In the analysis of real astronomical maps or surveys a similar approach can be adopted. Although the exact methods of carrying out the analysis are more sophisticated than the approach outlined here, the basic idea is the same. Figure 4.34 shows the results of a counts-in-cells analysis of a particular three-dimensional redshift survey of galaxies. (In fact, the galaxies were a subset of the PSC*z* survey that was mentioned above.) The observational data, which cover a range of scales from about 10 to 80 Mpc are shown by the red line in Figure 4.34. As might be expected, the relative variation decreases with length scale – such that for cells with sides of length 50 Mpc the relative variation is about 30%. The analysis that was carried out on the real data can also be applied to the results of simulations of the formation of large-scale structure. The results of the counts-in-cells analysis of one such theoretical model is shown as the blue line in Figure 4.34, and now we can start to see the power of this type of analysis. If a simulation produces a pattern of variation that is similar to that which is observed in the real Universe, then we might be able to discriminate between different scenarios under which structure formed in the Universe.

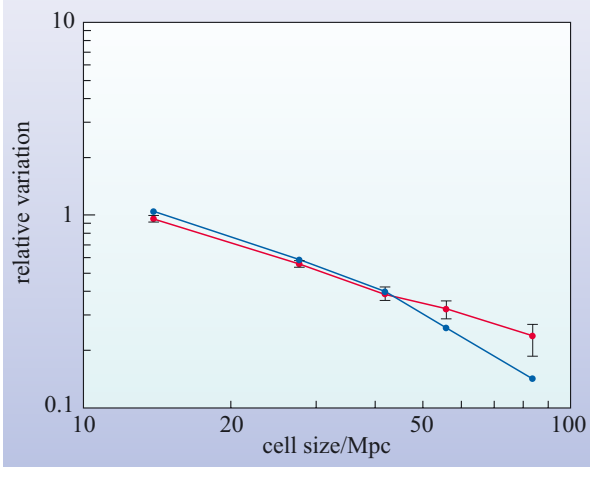

Figure 4.34 The results of a counts-in-cells analysis of three-dimensional survey data. The redshift survey was part of the program that constituted the PSC*z* survey (see Figure 4.18). The observational data are shown in red. The blue line shows the counts-in-cells results that would be expected from a particular model for the formation of structure. (Adapted from Oliver *et al*., 1996)

We won't dwell on the results of such comparisons here – since in order to put them into proper context, it is necessary to first develop the cosmological framework that we can use to describe the evolution of the Universe as a whole. However we will return to the topic of the formation of structure in Chapter 6. Furthermore, in Chapter 7 you will see how a similar type of analysis – which is based on characterizing the fluctuations in a map – is now enabling cosmologists to determine some of the fundamental physical parameters that describe the evolution of the Universe. In order to make further progress then, we need to consider how a scientific understanding of the Universe on the very largest scales has been developed; this is the subject of the next chapter.

4.7 Summary of Chapter 4

The large-scale distribution of galaxies

- Galaxies are gravitationally clustered into groups (containing up to about 50 galaxies) and clusters (which contain from about 50 to over a 1000 galaxies).
- Our Galaxy belongs to the Local Group of galaxies consisting of about 30 members but dominated by the Milky Way and Andromeda galaxy (M31).
- Medium-scale three-dimensional surveys confirm the existence of superclusters, loose collections of clusters which are about 30–50 Mpc in extent. Superclusters are not virialized systems.
- Our Local Group is at the outer edge of the Local Supercluster which is centred on, and dominated by the Virgo cluster.
- Redshifts can be combined with positions on the sky to obtain surveys of galaxies in three dimensions.
- The introduction of efficient electronic detectors and computer automation has resulted in a huge increase in the efficiency of redshift measurements. Current surveys are aimed at mapping large portions of the sky to great depth to look at the distribution of structure on scales of hundreds of megaparsecs.
- One method of describing of the large-scale cosmic structure is by using a counts-in-cells analysis. This quantifies how fluctuations in density vary with length scale. This allows comparisons to be made between the real distribution of galaxies and the results of numerical simulations of the formation of structure.

Clusters of galaxies

- Most clusters of galaxies have a radius of about 2 Mpc (the Abell radius). The mass of a typical cluster is of the order of 10^{14} to $10^{15} M_{\odot}$.
- Cluster masses can be estimated by three main methods: velocity dispersion, X-ray emission and gravitational lensing. The masses obtained by these methods typically agree within a factor of two or three.
- A cluster is said to be virialized if it is a gravitationally bound system and is in dynamical equilibrium. The mass of such a cluster can be obtained from the dispersion of the line of sight velocities (Δv) using $M \approx R_{\mathrm{A}}(\Delta v)^2/G$.
- Rich clusters are strong X-ray emitters due to the presence of hot intracluster gas. X-ray observations can be used to estimate the total mass of the cluster and the mass of X-ray emitting gas.
- A cluster can act as a gravitational lens of a distant galaxy, producing distorted multiple images. This is a means of detecting distant objects and can also be used to estimate the mass of the intervening cluster.
- Estimates of the masses of clusters from all three methods (virial theorem, X-ray emission and gravitational lensing) indicate that there is far more matter in clusters than the sum of the individual galaxy masses. This suggests the presence of dark matter in clusters. Typically galaxies will contribute less that about 10% of the mass of a cluster. The intracluster gas may constitute up to about 25% of the total mass. Dark matter makes up between 70% and 90% of the total mass of the cluster.

- X-ray spectra from clusters show that the hot intracluster medium contains an unexpectedly high metal content. This enrichment of the ICM is the result of supernova explosions in energetic young star-forming galaxies.
- Temperature maps of clusters indicate that many clusters are not in a state of hydrostatic equilibrium. This can give us information about the formation of clusters, and suggests that clusters may grow from the merging of smaller subclusters.

The intergalactic medium

- Some quasar spectra contain multiple absorption lines indicating the presence of gas (mainly neutral hydrogen) at different distances along the line of sight. This is called the Lyman α forest and can be used to detect the presence of neutral gas in the intergalactic medium.
- The absence of the Gunn–Peterson effect indicates that the density of any smooth neutral intergalactic medium must be very small out to large redshifts. Recent observations of very distant quasars ($z > 6$) are being used to look for the epoch of reionization using this effect.

The distribution of dark matter

- Dark matter forms the dominant contribution to the mass of clusters of galaxies (70–90%). Within clusters, the dark matter is distributed more smoothly than the matter that is present in the form of galaxies.
- The large-scale distribution of dark matter can be mapped by looking at small distortions in background galaxies – this effect is known as cosmic shear.

Questions

QUESTION 4.7

If the Universe is 13 billion years old, calculate the fraction of this age at which we see today (a) the Virgo cluster and (b) galaxies at the mean redshift of the galaxies in the SDSS.

QUESTION 4.8

Can you think why using Lyman α absorption spectra as a means to detect distant structure might give a biased view of the distribution of matter in the Universe? In particular, would you expect that Lyman α absorption would occur in regions where the density of galaxies is very high?

QUESTION 4.9

The masses of clusters of galaxies can be measured using methods based on three different physical processes. Name these methods and state what assumptions must be made about the physical state of the cluster in order for the individual methods to be applied.